Comprehensive Summaries of Uppsala Dissertations
from the Faculty of Science and Technology 774

The colour of gluon interactions

Studies of Quantum Chromodynamics in soft and hard processes

BY

NICUŞOR TÎMNEANU

ACTA UNIVERSITATIS UPSALIENSIS
UPPSALA 2002

Dissertation for the Degree of Doctor of Philosophy in Physics presented at Uppsala University in 2002

ABSTRACT

Tîmneanu, N. 2002. The colour of gluon interactions. Studies of Quantum Chromodynamics in soft and hard processes. Acta Universitatis Upsaliensis. *Comprehensive Summaries of Uppsala Dissertations from the Faculty of Science and Technology* 774. 64 pp. Uppsala. ISBN 91-554-5464-X.

Quantum Chromodynamics (QCD) is the theory of the strong interaction, one of the fundamental forces of nature. The interactions between quarks are mediated by gluons, which are the colour-charged gauge fields in QCD. Hard processes with a large momentum transfer can be calculated using perturbation theory, while soft processes with a small momentum transfer are poorly understood. In this thesis, various aspects of the gluon interactions are studied based on the interplay between hard and soft processes.

Soft gluon exchanges do not affect the dynamics of a hard process, but can rearrange the colour topology, resulting in different final states. The soft colour interaction models employ this idea and give a good description of all diffractive hard scattering data observed in $p\bar{p}$ collisions (W, Z, dijets, $b\bar{b}$, J/ψ). This thesis also presents predictions for diffractive Higgs and $\gamma\gamma$ production at present and future hadron colliders.

Multiple gluon exchanges give rise to saturation effects in hadronic collisions at high energies. Implementing this idea in photon-photon collisions gives new insight into the quantum structure of the photon and its interactions at high energies. When combined with perturbative calculations for single gluon exchange, the obtained results are in good agreement with experimental data from e^+e^- colliders.

Off-shell gluon distributions in the photon give another perspective on the photon structure and have been parameterized for the first time in this thesis. These are useful for calculating cross sections of processes where the effects of transverse momenta are crucial, for example heavy quark production in γp or $\gamma\gamma$ collisions.

Quantization of gauge fields which have a richer gauge structure than the gluons in QCD, is studied using the powerful BRST quantization formalism. Thus, first-stage reducible theories, like topological Yang-Mills and spin-5/2 gauge fields, are successfully quantized in an irreducible way.

Understanding gluon interactions and the interplay between soft and hard processes paves the way towards solving the longstanding problem of *confinement* in QCD.

Nicuşor Tîmneanu, Department of Radiation Sciences, High Energy Physics, Uppsala University, Box 535, SE-751 21 Uppsala, Sweden

ISSN 1104-232X
ISBN 91-554-5464-X
Printed in Sweden by Fyris-Tryck AB, Uppsala 2002

To the beloved ones

"Noli turbare circulos meos"
212 BC, Archimedes' legendary last words

Lesson on the circle

Draw a circle in the sand
then cut it in two,
with the same stick of hazel tree cut it in two.
After that fall to your knees,
after that fall to your hands.
After that strike your forehead against the sand
and ask the circle to forgive you.
That's it.

Lecţie despre cerc

Se desenează pe nisip un cerc
după care se taie în două,
cu acelaşi băţ de alun se taie în două.
După aceea se cade în genunchi,
după aceea se cade în brânci.
După aceea se izbeşte cu fruntea nisipul
şi i se cere iertare cercului.
Atât.

1979, Nichita Stănescu, Operele imperfecte

This thesis is based on the following papers:

I N. Tîmneanu and G. Ingelman,
Soft remnant interactions and rapidity gaps,
Deep Inelastic Scattering DIS2000 (2000) 586, hep-ph/0006227.

II R. Enberg, G. Ingelman and N. Tîmneanu,
Soft color interactions and diffractive hard scattering at the Fermilab Tevatron,
Physical Review D **64** (2001) 114015, hep-ph/0106246.

III N. Tîmneanu, R. Enberg and G. Ingelman,
Soft colour interactions and diffractive hard scattering at the Tevatron,
Journal of High Energy Physics Proceedings Section,
PrHEP-hep2001/051, hep-ph/0111210.

IV R. Enberg, G. Ingelman, A. Kissavos and N. Tîmneanu,
Diffractive Higgs boson production at the Fermilab Tevatron and the CERN Large Hadron Collider,
Physical Review Letters **89** (2002) 081801, hep-ph/0203267.

V N. Tîmneanu, R. Enberg and G. Ingelman,
Diffractive Higgs production: Soft colour interactions perspective,
Acta Physica Polonica B **33** (2002) 3479, hep-ph/0206147.

VI R. Enberg, G. Ingelman and N. Tîmneanu,
Diffractive Higgs and prompt photons at hadron colliders,
Submitted to Physical Review D, hep-ph/0210408.

VII N. Tîmneanu, J. Kwieciński and L. Motyka,
Saturation model for two-photon interactions at high energies,
European Physical Journal C **23** (2002) 513, hep-ph/0110409.

VIII N. Tîmneanu, J. Kwieciński and L. Motyka,
Saturation model for 2γ physics,
Acta Physica Polonica B **33** (2002) 3045, hep-ph/0206130.

IX L. Motyka and N. Tîmneanu,
Unintegrated gluon in the photon and heavy quark production,
Submitted to European Physical Journal C, hep-ph/0209029.

X C. Bizdadea, S. O. Saliu and E. N. Tîmneanu,
On the irreducible BRST quantization of spin-5/2 gauge fields,
Classical and Quantum Gravity **15** (1998) 501, hep-th/9911144.

XI C. Bizdadea, M. Iordache, S. O. Saliu and E. N. Tîmneanu,
An irreducible BRST approach of topological Yang-Mills theory,
Helvetica Physica Acta **71** (1998) 262.

Contents

Chapter 1

Introduction

1.1 What is the World made of?

This is one of the questions to which a child seeks the answer as the marvels of the world unveil in front of his curious eyes. It is also the question that mankind has pondered about for a long time, in its continuous pursuit of knowledge. The answers to this riddle have ranged from the simple solution offered by the ancient Greek schools of philosophy, which proposed air, water, fire and earth as the building blocks of nature, to the more complex, yet well structured table of elements proposed by Mendeleev. All the answers, in spite of their variety, show our quest to describe nature using fundamental building blocks and basic interactions among these.

Todays answer to the question combines the simplicity of the ancient Greek concept of the world with the quantitative edifice of Mendeleev: "The world is made of quarks and leptons." It is the modern particle physics and its successful Standard Model that provides us with this statement and represents man's current organized effort to answer the question. The fundamental building blocks of the Standard Model (SM) are the elementary particles, i.e. quarks and leptons (see Table 1.1). They come in three generations and have a multitude of intrinsic properties, like mass, spin, charge and other so called quantum numbers. The interaction between these particles is mediated by the force carriers (see Table 1.1), and there are four types of interactions: electromagnetic, weak, strong and gravitation. Although the Standard Model successfully incorporates the electromagnetic, weak and strong interaction into one theory, gravitation has not been consistently included.

All known elementary matter particles have spin 1/2. They are called fermions and obey Pauli's exclusion principle, according to which there can only be one fermion in a given quantum mechanical state. All force carriers have integer spin and are called bosons. Unlike the fermions, many bosons can share the same state having the same quantum numbers. Thus, the spin property provides a basic way of classifying particles and a rule for their arrangement in different quantum states. The other quantum numbers of the elementary particles describe the properties of these particles when interacting via the basic forces: the electric

Table 1.1: The Standard Model matter constituents and force carriers. The respective antiparticles have opposite charges. The electric charge is defined in such a way that the electron charge is -1. The third component of the weak isospin is presented, and for colour no charge (0), triplet (3) and octet (8) charges are given. All values are according to the Particle Data Group [1].

		Name		Mass [GeV]	Charges		
					electric	isospin	colour
Fermions – spin 1/2	**Leptons**	ν_e	el. neutrino	$< 10^{-8}$	0	$+1/2$	0
		e	electron	0.000511	-1	$-1/2$	0
		ν_μ	muon neutrino	< 0.0002	0	$+1/2$	0
		μ	muon	0.106	-1	$-1/2$	0
		ν_τ	tau neutrino	< 0.02	0	$+1/2$	0
		τ	tau	1.777	-1	$-1/2$	0
	Quarks	u	up	0.003	$+2/3$	$+1/2$	3
		d	down	0.006	$-1/3$	$-1/2$	3
		c	charm	1.3	$+2/3$	$+1/2$	3
		s	strange	0.1	$-1/3$	$-1/2$	3
		t	top	174.3	$+2/3$	$+1/2$	3
		b	bottom	4.3	$-1/3$	$-1/2$	3
Bosons spin 1		γ	photon	0	0	0	0
		Z^0	Z boson	91.19	0	0	0
		$W^\pm$	W boson	80.42	± 1	± 1	0
		g	gluon	0	0	0	8

charge is the source of electromagnetic interaction, the weak isospin is related to the weak interaction, the colour charge is the source for the strong force. The mass is generated in the Standard Model via the so called Higgs mechanism [2] and determines the strength of the gravitational force. Thus, one expects one more particle to be added to the above picture of elementary particles, the Higgs boson. It is the interaction with the Higgs boson that makes the other particles massive, yet the Higgs boson has not been observed so far [1].

The interactions that govern the matter particles, and implicitly their carriers, have quite different properties. The electromagnetic interaction, which couples to the electric charge of the particles, has an infinite range and is mediated by massless photons. The weak interaction, on the other hand, is carried by heavy bosons, called W and Z, and acts at very small distances of 10^{-18} meters. Although the strength of these two fundamental forces is different for processes in nature, the weak force being about 10 000 times weaker than the electromagnetic

[1] There is an experimental indication of Higgs boson with a mass of 115.6 GeV from the Large Electron-Positron (LEP) collider at CERN [3].

one, the two interactions have been unified into what is called the Electroweak Theory. The strength of the strong interaction is 100 times higher than the electromagnetic interaction, but the range is limited to about 10^{-15} meters. This interaction acts on the colour of the elementary particles and is mediated by gluons, which have no mass. The quarks are the only matter particles with non-zero colour. The theory describing the interactions between quarks and gluons is called Quantum Chromodynamics (from the Greek 'khroma', meaning colour).

In addition to these forces embedded in the Standard Model there is also gravitation. At the level of particle physics, the weakness of this force (10^{-39} smaller than the strong force) makes it insignificant compared to the other interactions and can be safely neglected. The carrier is believed to be a massless particle called graviton, and the range of this force is infinite. It is the goal of many physicists within the field of particle physics to incorporate all interactions into one unified theory.

How fundamental are these building blocks of matter? All particles in the Standard Model are point-like particles, having no observed substructure down to scales as low as 10^{-18} meters. At particle colliders, which are like huge microscopes that allow us to study the inner structure of matter, there has been a continuous race in the past few decades to increase the resolving power and investigate how elementary these particles are. The experimental evidence from these colliders gives us confidence in the Standard Model and its constituents (see Table 1.1).

For this picture to be complete, a mirror image containing the antiparticles needs to be supplemented. For each particle there is an antiparticle, which has the same mass and spin, but opposite values for the electric charge, weak isospin and colour. These antiparticles undergo the same fundamental interactions with the same strengths, as their matter partners.

Having received all "Lego" blocks of nature and different "glues" to put them together, the "child" can now proceed to build the World we live in. By adding quarks together and gluing them with gluons, hadrons can be formed, among them protons and neutrons (with sizes of 10^{-15} m). Binding these together with the remaining strong glue results in nuclei, which supplemented with electrons via the electromagnetic interaction give atoms, of typical size 10^{-10} m. From atoms, the step to molecules is made just by adding many of them and relying on the electromagnetic force to keep them together.

Living cells are made from atoms and molecules, and they can be as large as 10^{-5} m. Nature with the objects that surround us is made of these atoms, molecules and cells. At the macroscopic level in nature the gravitational force is felt. Not only does it keep us bound to the Earth, but it also keeps the Earth bound to the Sun, forming a system which is 10^{11} m large. This star gives us life by burning its fuel, a process where the weak interaction between quarks inside the protons and neutrons plays a crucial role.

1.2 A colourful theory

The two main ingredients of the Standard Model are the Electroweak Theory and Quantum Chromodynamics. While the former theory has managed to unify the electromagnetic and the weak interactions, the latter deals solely with the strong interactions. The Standard Model incorporates both these theories through the extended symmetry given by the U(1)×SU(2)×SU(3) group. The abelian gauge theory, invariant under transformations of the unitary group $U(1)_{em}$ is Quantum Electrodynamics. The Electroweak Theory adds the isospin SU(2) group to the symmetry $U(1)_Y$ hypercharge, and the symmetry $U(1)_Y \times SU(2)$ is broken to $U(1)_{em}$ by the mechanism of spontaneously symmetry breaking. The scalar Higgs boson and its interaction potential are responsible for this mechanism, which provides masses to the fermions. By adding one more group, SU(3) colour, the symmetry is extended and the Standard Model is set to include the strong interaction.

The path towards establishing Quantum Chromodynamics (QCD) as the theory of strong interactions was laborious and is worth mentioning. The interplay between the experimental observations and the theoretical advances was crucial in imposing a quantum field theory as a solution to the strong interactions of hadrons. Such an approach was generally disbelieved in the fifties and sixties, due to the failure of perturbative methods in describing the scattering theory of hadrons. Other approaches emerged in those days, such as Regge theory [4], which attempted to describe particles through the analytical properties of scattering amplitudes.

The suggestion that hadrons are not fundamental particles, but instead are composed of quarks, came in 1964 from Gell-Mann [5] and Zweig [6], as a result of the studies in hadron classification and their mass spectra. The quark model was born, with the term 'quark' adopted by Gell-Mann. The idea of a new quantum number [7, 8], later on called 'colour' by Gell-Mann, grew out of an attempt to avoid the apparent breaking of Pauli's principle, having quark spin 1/2 particles with the same quantum numbers forming a baryon.

The first series of high energy experiments, with the goal of probing the structure of hadrons, was initiated in the sixties at the Stanford Linear Accelerator Center (SLAC). The idea was to probe the hadron with a beam of structureless particles, like leptons. The same method was used by Rutherford half a century earlier when investigating the structure of atoms with, what he believed were structureless, α particles. In this way the field of Deep Inelastic electron-proton Scattering (DIS) started. The obtained experimental results [9] could be understood if one assumed that the electrons scatter on almost free point-like constituents in the proton, called partons, as proposed by Feynman [10] and Bjorken and Paschos [11] in 1969. Thus the parton model appeared, with Feynman coining the name 'parton'.

The scaling property of the proton structure functions, as proposed by Bjorken, was confirmed by the SLAC experiment. The interpretation of this scaling is that the constituents of the proton are free and point-like when observed with high

spatial resolution. The high resolution can be translated into a high momentum transfer from the incoming electron. A direct consequence is the fact that the interaction between partons becomes weaker at short distances. Finding a field theory which had this property was the next step.

It was back in 1954 when Yang and Mills [12] introduced a gauge theory which had a non-abelian (i.e. non-commutative) gauge symmetry. The generators of the symmetry group are non-commutative, and they form a Lie algebra. This non-abelian gauge field theory was successfully quantized by Faddeev and Popov [13] in 1967, and 't Hooft and Veltman [14] showed in 1971-1972 that such theories are also renormalizable. Thus, the original Yang-Mills theory had the ability of being quantized in a manner which was both unitary and renormalizable.

The breakthrough was provided in 1973, by Gross and Wilczek [15] and Politzer [16] who found the property of asymptotic freedom in the Yang-Mills theory. This means that the strength of the interaction is energy dependent, with the coupling strength becoming weaker at high energies (short distances). In other words, the parton model was rediscovered and the experimental results from SLAC could be understood from the field theory point of view.

It became clear that the dynamics of the quarks is described by non-abelian gauge field theories. The new symmetry, generated by the non-commutative algebra, was quickly accommodated with the use of the new quantum number colour, and the symmetry in the quark model (Fritzsch, Gell-Mann and Leutwyler [17]). The non-observation of isolated quarks was to be understood in a natural way within this symmetry, as well as other experimental findings, like the experimental data on the total cross-section for $e^+e^- \rightarrow hadrons$. The partons, having the same quantum numbers and properties as the quarks, could then be identified with quarks. The theory describing the strong interaction was finally established as 'Quantum Chromodynamics'.

The gluon (a term also introduced by Gell-Mann [18], however in the context of neutral vector theories) is the mediator of the strong force. It carries colour and it is self-interacting, a property which proved to be essential for the asymptotic freedom of QCD. The same property of gluon self-interaction was found to lie behind the confinement of quarks at long distances [19, 20]. This adds as an important property of QCD, which now combines the short distance physics represented by asymptotic freedom with long distance phenomena, like quark confinement. However, QCD does not provide a single approximation method which is applicable to all length scales.

With the advent of asymptotic freedom, perturbative Quantum Chromodynamics (pQCD) was born, imposing perturbation theory as a tool which can be safely used to describe short distance reactions. Asymptotic freedom is after all a perturbative prediction, while on the other hand, confinement is not. The first attempts in pQCD were to recover Bjorken scaling, and violation of this scaling was found due to QCD corrections [21, 22]. The experimental observation of such violations [23] in muon-nucleon scattering, gave strong support to perturbative QCD.

From this moment on, the field of perturbative QCD has been flourishing.

The introduction of operator product expansion (OPE) [24] provided a powerful tool to extract the short-distance part in deep inelastic scattering. Perturbative calculations were made for total cross sections in e^+e^- collisions at leading order, and going even to next-to-leading order. The discovery of heavy quarkonia, which are bound states of heavy quarks, such as the J/ψ (charm) [25] and Υ (bottom) [26], came right after the foundation of QCD, and their decays were successfully described by QCD [27]. The concept of hadronic jets appeared [28], with jets coming from quarks or gluons, and QCD notably described these. The first evidence for gluons was found at Deutsches Elektronen-Synchrotron (DESY) [29] from hadronic jets.

The justification for the use of pQCD lies primarily with experiment. Perturbative QCD has developed in the area of high energy collisions, at large momentum transfers. At small momentum transfers using perturbative methods is problematic, as the gap between short distance phenomena and large distance phenomena needs to be passed. After all, the experiments testing QCD start from a short distance interaction and go towards large length scales, a transition during which the strength of the coupling grows. It became clear that QCD possesses an 'open' problem, namely how to understand properly the large distance phenomena, referred to as non-perturbative.

In spite of its continuous 'open' problem, QCD made its way as an integrant part of the Standard Model of elementary particles and their interactions. Quantum Chromodynamics is now-a-days regarded as one of the cornerstones of the Standard Model. It should also be mentioned that numerical studies of QCD based on a lattice formulation of the theory [30, 31, 32] added confidence to this theory of strong interactions.

The scope of this thesis is to explore the realm of QCD in general, and in particular, to deepen the understanding of non-perturbative QCD. In order to explore different aspects of gluon interactions, the approach taken is to use the basis of perturbative QCD to investigate long distance phenomena, relying on the interplay between the so called soft, long distance physics and hard, short distance physics.

The thesis is organized as follows. In chapter 2 the main elements of Quantum Chromodynamics are reviewed, starting with the basics of QCD as a quantum field theory, the perturbative QCD approach and the issues of non-perturbative physics. Chapter 3 introduces the interplay between hard and soft processes in QCD and the construction and properties of several phenomenological models that are used. In chapter 4, a short introduction to a powerful quantization method is given, as well as its relevance for quantum field theories, and in particular QCD. The summary of the papers on which the thesis is based can be found in chapter 5. Finally, chapter 6 contains the conclusions and an outlook.

Throughout the thesis, the natural units have been used, $\hbar = c = 1$. Thus, mass, momentum and energy are expressed in the same unit, which is GeV. Time and length have units of inverse energy, normally GeV^{-1}. The conversion to ordinary units can be made by using the appropriate factors of $\hbar = 6.582\,118 \times 10^{-25}$ GeV·s and $c = 299\,792\,458$ m·s^{-1}.

Chapter 2

Basics of Quantum Chromodynamics

This chapter gives a short overview of Quantum Chromodynamics, introducing the basic elements of QCD which are important for this thesis. For a thorough study, the following reviews and books are recommended [33, 34, 35, 36] to the interested reader. Certain basic concepts of relativistic quantum mechanics and Quantum Electrodynamics (QED) are assumed to be known, and this thesis does not make an effort in introducing or motivating them.

2.1 Fundamentals of QCD

Quantum Chromodynamics is a field theory which describes the strong interaction between the quarks and gluons. It is generally assumed that all fundamental particles (among them quarks and gluons) are represented by local quantum fields. In particle physics there is a consensus to describe all local fields by quantum field theories, and QCD is one such theory.

QCD, in its attempt to describe the strong interactions, introduces the concept of quarks and colour. The quark fields represent the matter fields, and although they are not directly observable, they form hadrons which are observed in nature. In order to describe this observation, QCD is based on the non-abelian SU(3) symmetry, and as a result the quarks have three charges, called colours. The physical observables are invariant under a global symmetry of the colour SU(3) group. Requiring the same invariance for local transformations of colour, gives eight massless gauge fields called gluons, that mediate the strong force. The gluons also carry colour, which makes them self-interacting. In the following, these important properties of QCD will become clear from the detailed construction of the theory.

The QCD Lagrangian

The starting point of QCD is the classical action, written as a functional of the

fields

$$S_0[\psi_f, \bar{\psi}_f, A^a_\mu] = \int d^4x \mathscr{L}_{classic}(\psi_f, \bar{\psi}_f, A^a_\mu; g, m_f), \tag{2.1}$$

where $\mathscr{L}_{classic}$ is the Lagrangian density, containing all the fields and the parameters of the theory. The fermionic fields $\psi_f(x)$ and $\bar{\psi}_f(x)$ describe the quarks and antiquarks, and the bosonic fields $A^a_\mu(x)$ describe the gluons. Different quark flavours are represented in the Lagrangian density via the label f. Furthermore, the parameters of the theory embedded in the density $\mathscr{L}_{classic}$ are the strength g of the coupling describing the interaction between quarks and gluons, and the masses m_f of the different quark flavours. All quark flavours are taken into account, so f is an index running from 1 to $N_f = 6$.

The classical Lagrangian density of QCD, based on the non-abelian Lagrangian originally written down by Yang and Mills [12], is given by

$$\mathscr{L}_{classic} = \sum_{f=1}^{N_f} \bar{\psi}_f (i\gamma^\mu D_\mu - m_f)\psi_f - \frac{1}{4} F^a_{\mu\nu} F^{\mu\nu}{}_a, \tag{2.2}$$

where the covariant derivative and the field strength are introduced as

$$D_\mu = \partial_\mu + igT_a A^a_\mu, \tag{2.3}$$

$$F^a_{\mu\nu} = \partial_\mu A^a_\nu - \partial_\nu A^a_\mu - g f^a{}_{bc} A^b_\mu A^c_\nu. \tag{2.4}$$

In the above, γ^μ are the Dirac matrices and $\partial_\mu = \frac{\partial}{\partial x^\mu}$. The rest of the used notations will become clear in the following discussion, which will introduce different key concepts in QCD.

The Lagrangian density has the crucial property of being invariant under local gauge transformations. Gauge invariance means that one can perform a redefinition of the colour quark fields independently at every point in space and time, without changing the physical content of the theory.

These gauge transformations define a group, called the $SU(3)$ group (3 stands for the number of colours). In general, this group is denoted $SU(N_c)$, and one can keep track of the number of colours N_c in the theory. There are $N_c^2 - 1 = 8$ generators of this group, T_a with $a = 1 \dots N_c^2 - 1$. These do not commute with each other, but satisfy the following relation

$$[T_a, T_b] = i f_{abc} T^c, \tag{2.5}$$

which defines a Lie algebra with the structure constants f_{abc} of $SU(3)$.

With the help of these generators, the covariant derivative D_μ acting on the spinor quark fields, is introduced. The field strength $F^a_{\mu\nu}$ is defined in terms of the gluon vector fields A^a_μ and the structure constants of the SU(3) algebra. Under a local gauge transformation $\mathcal{U}(x) = \exp(-ig\epsilon^a(x)T_a)$, the different transformation rules of the fields are

$$\psi_f(x) \rightarrow \psi'_f(x) = \mathcal{U}(x)\psi_f(x), \tag{2.6}$$

$$\mathbf{A}_\mu(x) = A^a_\mu(x)T_a \rightarrow \mathbf{A}'_\mu(x) = \mathcal{U}(x)\left(\mathbf{A}_\mu(x) - \frac{i}{g}\partial_\mu\right)\mathcal{U}^{-1}(x), \tag{2.7}$$

$$\mathbf{F}_{\mu\nu}(x) = F^a_{\mu\nu}(x)T_a \rightarrow \mathbf{F}'_{\mu\nu}(x) = \mathcal{U}(x)\mathbf{F}_{\mu\nu}(x)\mathcal{U}^{-1}(x), \tag{2.8}$$

where $\epsilon^a(x)$ are arbitrary real functions defined at any point in space-time x. The field strength tensor $F^a_{\mu\nu}$ is not invariant under the gauge transformations. This behaviour is given by the non-abelian character of QCD, and should be contrasted with that of the electromagnetic field in QED, which is invariant. More important is that the Lagrangian density and the action are invariant under the gauge transformations, which can be easily checked using the formulae above.

The Lagrangian density is formed of several important pieces. It contains the term $\bar{\psi}_f(i\gamma^\mu\partial_\mu - m_f)\psi_f$, which describes the free quark fields, as well as factors of the type $\partial_\mu A^a_\nu \cdot \partial^\mu A^\nu{}_a$, describing the free gluonic field. The rest of the terms in the Lagrangian represent the interaction between the quark fields and the gluon fields $g\bar{\psi}_f\gamma^\mu T_a A^a_\mu\psi_f$, or the interaction of the gluon fields among themselves $gf_{abc}A^a_\mu A^b_\nu(\partial^\mu A^{\nu c})$ and $g^2 f_{abc}f^a{}_{ed}A^b_\mu A^c_\nu A^{\mu e}A^{\nu d}$. This shows that the parameter g of the theory controls the coupling of the interaction between quarks and gluons. Furthermore, the latter terms show explicitly the self-interaction of the gluon, which is an important property of QCD.

Other properties of QCD can be explored at the classical level. For example, using the principle of least action, the equations of motions can be derived. The quark fields will obey a Dirac-type equation

$$(i\gamma^\mu D_\mu - m)\psi_f(x) = 0, \tag{2.9}$$

while for the gluon fields the following equations of motion can be obtained

$$D_\mu{}^a{}_b F^{\mu\nu}{}_a = g\bar{\psi}_f\gamma^\nu T_b\psi_f\,, \tag{2.10}$$

where $D_\mu{}^a{}_b$ represents the covariant derivative in the adjoint representation. These equations are similar to Maxwell's equations for the electromagnetic field, but they describe the non-abelian colour field of QCD, where the righthand-side gives the quark colour sources.

Quantizing QCD

The next step in the construction of a quantum theory for quarks and gluons is to quantize the above Lagrangian. The quantization of a theory is not a unique procedure, and there are a variety of quantization methods which lead to the same physical predictions. For example, one can use the canonical operator formalism introduced by Heisenberg and Pauli [37], or the functional-integral formalism introduced by Feynman [38]. The latter formalism has the advantage that the classical Lagrangian appears in the functional integral, which makes it convenient to deal with its symmetries, like the gauge symmetries.

There are some difficulties in making a straightforward quantization of the classical Lagrangian (2.2) due to its gauge invariance. The action (2.1), which is used to construct the generating functional, does not depend on all of the components of the gauge fields, which is a direct consequence of the fact that the action itself is invariant under gauge transformations, $S_0[\psi'_f, \bar{\psi}'_f, A'^a_\mu] = S_0[\psi_f, \bar{\psi}_f, A^a_\mu]$. This means that when constructing the path integral

$$Z[0] = \int \mathcal{D}\psi_f\mathcal{D}\bar{\psi}_f\mathcal{D}A^a_\mu\; e^{iS_0}, \tag{2.11}$$

there will be an overcounting of the degrees of freedom by integrating over fields which are connected via gauge transformations, and this integral will become infinite. This implies, for example, that defining a propagator for the gluon field makes no sense.

The solution to this problem is to introduce a convention for fixing the gauge invariance through a gauge-fixing term. The physical results will not depend on the way the gauge is fixed. Furthermore, the extra degrees of freedom can be effectively cancelled by introducing new fields, called ghost fields [13]. Thus, the QCD Lagrangian will have the following form

$$\mathscr{L}^{QCD}(\psi_f, \bar{\psi}_f, A^\mu, \eta, \bar{\eta}) = \mathscr{L}_{classic} + \mathscr{L}_{gauge-fix} + \mathscr{L}_{ghost}. \tag{2.12}$$

The form of $\mathscr{L}_{gauge-fix}$ can be chosen freely, and one common choice is the covariant gauge

$$\mathscr{L}_{gauge-fix} = -\frac{1}{2\xi}(\partial^\mu A^a_\mu)^2, \tag{2.13}$$

where ξ is an arbitrary constant. If this gauge-fixing term is imposed, then the following ghost term needs to be added

$$\mathscr{L}_{ghost} = (\partial_\mu \bar{\eta}_a)(\partial^\mu \delta^a{}_c - g f^a{}_{bc} A^b_\mu)\eta^c. \tag{2.14}$$

This term introduces new fields, $\eta^a(x)$ and $\bar{\eta}_a(x)$, which are the ghost and antighost fields. These fields do not correspond to physical particles, but are fictious fields which will enable later perturbative calculations. These fields are scalar fields and have both fermionic characteristics, in the sense that they obey Fermi statistics, and bosonic ones, having a bosonic-like propagator.

As seen in Eq. (2.14) for the choice of covariant gauge, the ghost fields couple to the gluon fields, which is not the case in QED. The covariant gauge fixing has the advantage of providing a simple form for the gluon propagators. One can choose other gauge-fixing procedures, like the axial gauge, which has the advantage of decoupling the ghosts from the gluons, thus eliminating the ghost fields from the calculations, at the expense of a complicated gluon propagator.

At this point, the quantization of QCD is complete, and one can write the functional integral

$$Z[0] = \int \mathcal{D}\psi_f \mathcal{D}\bar{\psi}_f \mathcal{D}A^a_\mu \mathcal{D}\eta_a \mathcal{D}\bar{\eta}_a \exp\left\{(i \int d^4x \mathscr{L}^{QCD}(\psi_f, \bar{\psi}_f, A^\mu, \eta, \bar{\eta})\right\}. \tag{2.15}$$

which represents the central piece for performing calculations in QCD. Without expanding into details, the above path integral is used to construct the so called generating functional $Z[J]$, which contains external source functions $J(x)$. With the help of this functional integral, all the Green functions can be generated. These are the same Green functions that can be obtained using the canonical quantization procedure, representing the vacuum expectation value of the time-ordered product of field operators.

The Green functions supply the route towards experimentally observable quantities. The Green functions themselves are not direct physical observables, but

are related to the cross-section in the following way [39]. The scattering matrix, called the S matrix, describes the amplitude for the scattering of two incoming particles into several outgoing particles. From the Green functions one can derive the S matrix, which in turn can be used to calculate the cross section describing the scattering of the two incoming particles. The decay widths of particles can be calculated in a similar manner.

In this way, QCD can provide predictions for the scattering of particles, which can be tested experimentally in high energy particle collisions.

2.2 Perturbative QCD approach

The final statement in the previous section may seem promising, providing a simple way to test the validity of QCD, however, the situation is more complicated. If the particles corresponding to the fields are observable, like leptons and photons in the case of QED, the above formalism can simply be applied to calculate scattering cross sections for these particles. In QCD, however, the quarks and gluons are confined and cannot be observed in an isolated state. The only observable particles are the hadrons, composed of quarks and gluons, and only scattering experiments with hadrons (and leptons) can be performed. Thus, a method has to be employed, for obtaining the scattering cross section of hadrons from the quark Green function. Such a method should involve the treatment of non-perturbative QCD, as will be discussed later.

Feynman rules

Since QCD is a theory with interactions, it is not straightforward to solve it. Even at the classical level, the equations of motion (2.9) and (2.10) cannot be solved exactly due to the interaction terms coupling the quarks and gluons. The same problem is encountered at the quantum level, when calculating the Green functions. In the case of a free field theory (with no interactions) it is possible to evaluate the generating functional exactly, and subsequently the Green functions. When interactions are added, the generating functional can no longer be evaluated exactly, and a way out is provided by perturbation theory.

As seen in Sec. 2.1, the interaction terms in the QCD Lagrangian are all controlled by the parameter g of the theory, called the coupling. It is customary in QCD to work with the following notation

$$\alpha_s \equiv \frac{g^2}{4\pi}, \tag{2.16}$$

defining the strong coupling. When this coupling is small, the interactions can be considered as perturbations on the free field solution. The smallness of this parameter provides a way of expanding the generating functional in powers of the coupling, thus allowing approximate calculations, order by order.

The first step would be to separate the Lagrangian density of QCD $\mathscr{L}^{QCD}$ into two pieces, a free piece $\mathscr{L}_0$ which contains all the terms bilinear in the fields,

and an interaction piece $\mathscr{L}_I$ which contains the rest. The QCD action will have the form

$$S^{QCD} = S_0 + S_I = \int d^4x \mathscr{L}_0 + \int d^4x \mathscr{L}_I \tag{2.17}$$

From the free action S_0, the 2-point Green function can be calculated, corresponding to the free field solution. The 2-point Green function is called a propagator, and represents the propagation of the particle between two space-time points.

It is customary to depict the Green functions using the so called Feynman diagrammatic. The Feynman diagrams, as will be seen later, offer an intuitive view of the interactions and processes between particles, as well as a recipe for performing perturbative calculations. In such a representation, the free particles propagating are represented by lines. The quarks are illustrated with straight lines, whereas the gluons are illustrated with curly lines. For ghosts, present for instance in covariant gauges, a dashed line is used. The arrow on the fermionic lines shows the flow of the momentum, k.

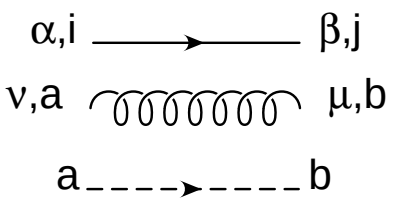

$$i\delta_{ij}\frac{[k+m]_{\beta\alpha}}{k^2-m^2+i\epsilon}$$

$$i\delta_{ab}\frac{1}{k^2+i\epsilon}\left[-g^{\mu\nu}+(1-\xi)\frac{k^\mu k^\nu}{k^2+i\epsilon}\right]$$

$$i\delta_{ab}\frac{1}{k^2+i\epsilon}$$

Figure 2.1: Feynman rules for the propagators in QCD: quark, gluon and ghost.

The second piece of the action, S_I, which contains all the interactions between the fields, is proportional to the coupling parameter g. With our assumption of a small coupling, S_I can be treated as a perturbation and the Green functions of the interacting theory can be calculated. These Green functions are called vertices, and they represent the interaction between particles which propagate freely towards and from the interaction point. These vertices form a set of Feynman rules, like the propagators, and they are represented by points where three or more lines meet. Although not written explicitly here, it should be noted that all vertices from Fig. 2.2 are proportional to the coupling g, except the 4-gluon vertex which is proportional to g^2.

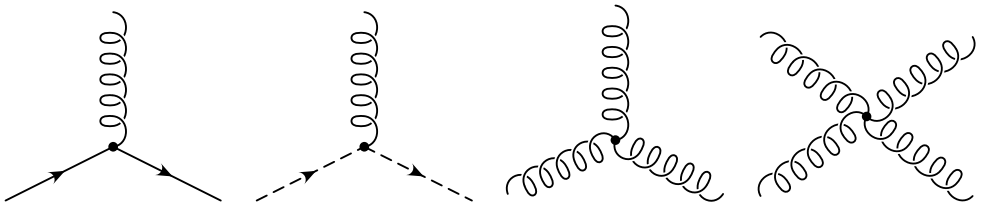

Figure 2.2: Vertices describing the interaction between fields in QCD.

In order to obtain transition matrix elements, the above set needs to be supplemented with rules for the external lines. The external particles are assumed to be on the mass shell. This can be done by adding the spin wave functions for the external fermions,*i.e.* the Dirac spinors $u(p)$ and $v(p)$, or the polarization vector $\epsilon^{\mu}(k)$ for the external gluons. There are no external ghost lines. It should be stressed that, since quarks and gluons are confined in hadrons, it is meaningless to consider free on-shell states for them. It is convenient, however, to treat quarks and gluons in approximate calculations as if they were in free states. Asymptotic freedom, which will be introduced later, guarantees that quarks and gluons are almost free at the short distances relevant for the interactions at high momentum transfer, thus allowing the use of free on-shell states.

Based on the above fundamental vertices and propagators, all reaction amplitudes can be computed in perturbative QCD using the Feynman rules. These rules are derived from the QCD action as shown above, and define a way of translating diagrams for the reactions into mathematical formulae. Also, additional rules, like loop sign factors and symmetry factors, should be added. The first additional rule takes into account the fact that the quarks and ghosts obey the Pauli principle. Introducing the symmetry factors gives a way to account for the bosonic nature of the gluons, which cannot be distinguished if they are in the same state.

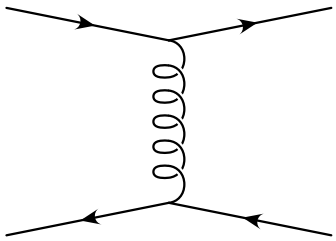

Figure 2.3: QCD Feynman diagram for quark-antiquark scattering amplitude.

The Feynman diagrams show the reaction in momentum space, where all lines defining particles have well defined momenta, and are not literary pictures of the reaction which takes place in ordinary space. Figure 2.3 shows an example of a Feynman diagram for the quark-antiquark scattering via a gluon exchange. The antiquarks are represented by the same lines as the quarks, however the arrows represent a propagation of the particles backwards in time. The time axis is going from left to right.

The Feynman rules offer a systematic way of calculating order by order the Green functions. Via these, the reaction cross sections can be obtained by squaring the sum of all scattering amplitudes which have the same initial and final configuration. The lowest-order calculation of a quark-gluon process corresponds to what is called a tree diagram, like the one in Fig. 2.3. Counting the coupling in the vertices, one finds that the amplitude for the above diagram has the order g^2, or α_s. Higher order diagrams will contain more vertices, which means they

will correspond to higher powers of α_s. One such example can be seen in Fig. 2.4, which involves a loop. Including all relevant diagrams it is possible to compute the cross section $\sigma(p)$ for any reaction as the square of all contributing amplitudes, where p is a generic notation for the momenta of all the particles involved. The perturbative expansion of this cross section can be written

$$\sigma(p) = a_1(p)\alpha_s^2 + a_2(p)\alpha_s^3 + ... \ , \tag{2.18}$$

where $a_1, a_2, ...$ are the coefficients computed at each order.

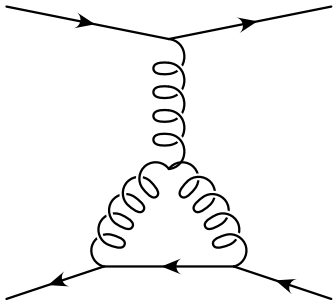

Figure 2.4: Example of a higher order Feynman diagram for quark-antiquark scattering.

Renormalizing QCD

The dynamical effects of QCD due to the gluon self-interaction, show up already at the tree level. These effects are also seen at higher orders, when QCD radiative corrections are added. However, such diagrams generate divergencies and this can be understood from Fig. 2.4. The internal loop has an arbitrary momentum, unlike the other legs or propagators which have well defined momenta, and integrating over this momentum will give infinity.

In order to obtain a finite result, which should correspond to the finite physical observables, these divergencies need to be subtracted. This subtraction is achieved by renormalizing the theory, and QCD was shown to be a renormalizable theory [14]. The first step is to require that the divergent integrals that arise in the theory are mathematically manageable, and to introduce a device that will separate the infinities from the finite results. This procedure is generically called regularization, and it is not a unique procedure, *i.e.* there exist a variety of regularization schemes.

All Green functions need to be regularized, like the propagators and vertices given above. For example, in the case of the gluon propagator, one can calculate the so called gluon self-energy. The relevant diagrams contributing to the gluon self-energy are shown in Fig 2.5. Dimensional regularization is one of the useful regularization schemes that can be used to regularize these diagrams. The diagrams 2.5bc are special for QCD due to the self-interacting gluon fields, and are not encountered for the photon in QED.

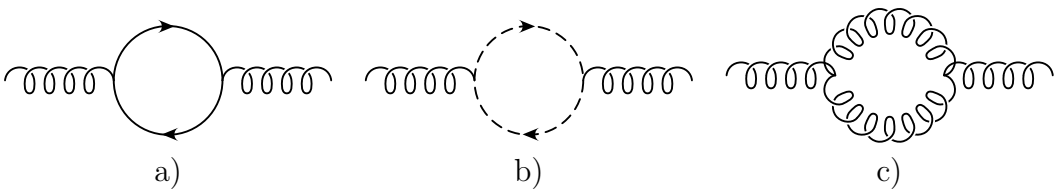

Figure 2.5: Diagrams contributing to the gluon self-energy.

Elimination of the infinities is done by shifting the fields and the parameters in the Lagrangian, in such a way to absorb these infinities. The parameters of the theory are in fact experimentally measurable and they are finite. The shifts in the coupling α_s and the masses m_f are motivated by the higher order contributions to the quark propagators (containing m_f) and quark-gluon vertex (containing g), contributions that yield infinities. After renormalizing the parameters and the fields, a renormalized Lagrangian is obtained. This new Lagrangian has the same form and symmetries as the original QCD Lagrangian and should be used as the starting point for calculating scattering processes to obtain finite results.

Asymptotic freedom

It should be noted that there is an arbitrariness in how to define a divergent piece and how much of the finite piece is to be extracted together with the infinity. Furthermore, this subtraction inevitably introduces an arbitrary mass scale μ, called the renormalization scale. One simple way to understand why such a scale appears, is to realise that the divergent loop integral can be limited with an upper cut-off on the momentum, thus providing the mass scale. A possible interpretation of such a regularization is that the theory is expected to break down at that scale, where new physics may enter.

The computed cross section will then have a new dependence, $\sigma(p, \mu^2)$, as well as its contributions at different orders, $a_n(p, \mu^2)$. Since $\sigma(p, \mu^2)$ describes unique physical phenomena, it should not depend on the choice of renormalization scheme, or the renormalization scale μ, so one can write

$$\mu^2 \frac{d}{d\mu^2} \sigma(p, \mu^2) = 0 \ . \tag{2.19}$$

This means that different renormalizations schemes have to be equivalent, and requiring such an equivalence gives a relation between different schemes that mathematically form a group, called the renormalization group [40, 41].

From the same arguments it follows that the renormalized coupling α_s depends on the choice made for the renormalized scale μ. Starting from Eq. (2.19) and from the perturbative expansion of $\sigma(p, \mu^2)$ given in Eq. (2.18), one can obtain the following scale dependence

$$\mu^2 \frac{d}{d\mu^2} \alpha_s(\mu^2) \equiv \beta(\alpha_s) = -\beta_0 \alpha_s^2 - \beta_1 \alpha_s^3 - ... \ , \tag{2.20}$$

This equation represents the renormalization group equation for the coupling. It introduces the β-function, which can be calculated perturbatively, and the first two coefficients have the following expression

$$\beta_0 = \frac{11N_c - 2N_f}{12\pi}, \tag{2.21}$$

$$\beta_1 = \frac{17N_c^2 - 5N_cN_f - 3C_FN_f}{24\pi^2}, \tag{2.22}$$

where N_c is the number of colours, N_f is the number of flavours and $C_F = (N_c^2 - 1)/2N_c$ is the value of the Casimir operator for the fundamental representation.

The solution of Eq. (2.20) is known as the effective or running coupling. In the leading order, the solution for the running coupling is given by

$$\alpha_s(\mu^2) = \frac{1}{\beta_0 \ln(\mu^2/\Lambda^2)}, \tag{2.23}$$

where Λ is the QCD scale parameter. Λ indicates the scale at which the coupling $\alpha_s(\mu^2)$ becomes strong, and the perturbative approach would fail.

The property of asymptotic freedom can easily be seen from the running coupling solution. As the scale μ increases, the coupling decreases. This means that for high energy scattering, where the large momentum transfer gives the scale of the scattering, the running coupling is small. If the coupling is small, perturbation theory can be performed successfully. It also means that the quarks and gluons, at these high momentum transfers, are weakly bound and behave like almost free particles.

The origin of asymptotic freedom can now be understood more easily. The self-interaction between the gluons is the basic reason for the asymptotic freedom. The diagram 2.5c contributes significantly to the value of β_0 and ensures that $\beta_0 > 0$. This type of diagram does not exist in QED, and that makes the corresponding value of β_0 negative, hence the lack of asymptotic freedom in this theory. Instead, in QED, the electromagnetic coupling α_{em} becomes stronger as the energy scale increases, and the effect of 'screening' of an electric charge is present. In QCD, asymptotic freedom can be thought of as 'antiscreening', *i.e.* the colour charge of the quarks is not screened by the gluons, which 'leak' away from the source. In this way, for high spatial resolution, the quarks become almost free.

The parton model

How can scattering cross sections for hadrons be constructed from the ones calculated using quarks and gluons? Asymptotic freedom provides now the answer: "perturbation theory". Within perturbation theory, the analysis of hadronic processes can be formally made using the operator product expansion (OPE) [24]. OPE is a powerful tool for extracting the quark-gluon interactions from hadrons. The parton model [10,11], however, gives a more intuitive feeling of the connection between hadrons and quark-gluon Green functions.

The parton model was born as a response to the observation of scaling, discovered at SLAC [9] in Deep Inelastic electron-proton Scattering (DIS). The experiment was set to investigate the structure of the proton, which afterwards was described with the so called structure functions. In the first measurements, it was observed that the structure functions were approximately independent of the scale $Q^2 = -q^2$ at which the proton was probed, where q is the momentum of the exchanged photon. This property, predicted in [11], can be seen as a consequence of the scattering on charged pointlike constituents in the proton. These constituents are called partons [10], and they are illustrated in Fig. 2.6.

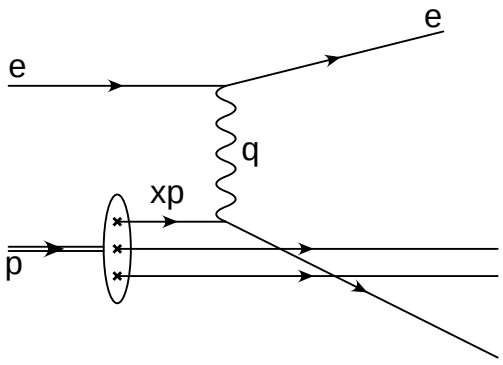

Figure 2.6: Schematic representation of deep inelastic scattering in the parton model. The electron strikes out a parton from the proton.

In the parton model, it is assumed that any physically observed hadron is made up of partons, which later on have been identified with quarks and gluons. In the infinite momentum frame, every relevant parton entering a scattering has an initial momentum xp, representing a fraction x of the longitudinal momentum p carried by the initial state hadron. In this way, the total cross section for DIS can be calculated based on only tree diagrams and some probability densities

$$\sigma(p,q) = \sum_i \int_0^1 dx\, \hat{\sigma}_i(xp,q) f_i(x) \ . \tag{2.24}$$

Here, $\hat{\sigma}_i(xp,q)$ represents the cross sections for interaction with the individual parton i, and $f_i(x)$ gives the probability density for finding the parton i inside the hadron, carrying the momentum fraction x, $0 < x < 1$.

In the case of collisions between two hadrons having momenta p_1 and p_2 (Fig. 2.7), the cross section can be written in a similar way. The cross section contains the parton distribution for each hadron convoluted with the cross section for the scattering of two partons i and j

$$\sigma(p_1,p_2) = \sum_{i,j} \int_0^1 dx_1 dx_2\, \hat{\sigma}_{ij}(x_1p_1, x_2p_2) f_i(x_1) f_j(x_2) \ . \tag{2.25}$$

The parton cross sections $\hat{\sigma}_{ij}$ can be calculated as mentioned earlier in perturbation theory, from the tree diagrams.

The physical features of the parton model are easily understood in DIS, from Fig. 2.6. Because of the high energy, in the center of mass system the proton suffers both a Lorentz contraction and a time dilation. The life time of the partonic state is thus much larger than the time it takes for the electron to cross the proton. Therefore, the electron sees a collection of 'frozen' partons as it passes the proton. Furthermore, the scale of the probe Q^2 is high, translating into a high spatial resolution. This makes it possible to write the cross section as the probability of finding a single parton times the cross section for the interaction with the parton (as in Eq. (2.24)).

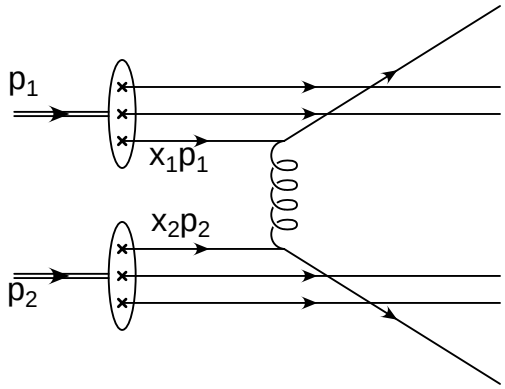

Figure 2.7: The collision of two hadrons represented schematically in the parton model. The hard interaction happens between two partons in the hadrons.

After the hard interaction, the different fragments of the proton interact. Due to the confinement of the quarks and gluons, only observable hadrons will emerge in a process called hadronization. This process happens too late to play a role in the electron-parton scattering, and it has a long time scale compared to the hard scattering. The parton model does not attempt to solve the problem of hadron binding. Instead, this information (the parton densities $f_i(x)$) is extracted from experiment, or it can be modelled [42].

Evolution equations

So far, in the description of the parton model, only the lowest order diagrams have been considered. Going beyond the lowest order, which in the DIS case was a pure electromagnetic process, means introducing QCD corrections. A simple way to analyse the effect of QCD corrections would be to consider the case of gluon emissions from a parton.

In the parton model, it is assumed that the partons have no transverse momentum. If the parton emits a gluon, it can acquire a transverse momentum k_t, with a probability proportional to $\alpha_s dk_t^2/k_t^2$. This momentum can extend up to the kinematic limit given by the probe Q^2, and will give contributions proportional to $\alpha_s \log Q^2$ when integrated over. These $\log Q^2$ effects are are induced by QCD and they break the scaling given by the naive parton model. Such scaling

violations have been observed experimentally (first time in [23]) and they show that hadron structure functions have indeed a dependence on the scale Q^2.

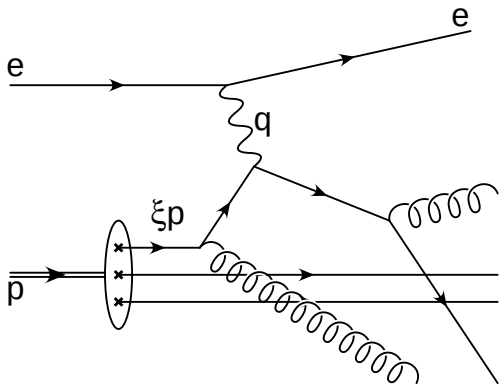

Figure 2.8: Deep inelastic scattering in the QCD-improved parton model.

The QCD corrections can be calculated in perturbation theory, and introduced in the parton model. One problem arises, however, given by divergencies in some of the diagrams that contribute, called collinear divergencies. These correspond to the limit $k_t^2 \to 0$, which represents the long range part in strong interactions, not calculable in pQCD. From the regularization of these infinities, in the same fashion as presented earlier for the case of renormalizing QCD, a new scale emerges. This scale is called the factorization scale μ_F, and basically represents the scale where the perturbative physics factorizes from the non-perturbative part. These infinities will be absorbed into the parton densities $f_i(x, \mu_F^2)$ at the scale μ_F.

Thus one can write the cross section with the scale dependent parton densities

$$\sigma(p, q, \mu_F^2) = \sum_i \int_0^1 d\xi \, \hat{\sigma}_i(\xi p, q) f_i(\xi, \mu_F^2) \ . \tag{2.26}$$

The factorization of the cross section into the two pieces, $\hat{\sigma}_i(\xi p, q)$ and $f_i(\xi, \mu_F)$, introduces a dependence on the factorization scheme which is similar to the renormalization scheme dependence described earlier. The choice of factorization scale μ_F is arbitrary, just as the renormalization scale μ. Also, the parton densities have been renormalized in a similar way as the strong coupling α_s.

The important observation is that all observable quantities do not depend on the choice of the factorization scheme or scale. For $\sigma(p, q, \mu_F^2)$, an equation similar to Eq. (2.19) can be written. From this, the scale dependence of the parton densities can be obtained at not too small x, giving the so called Dokshitzer-Gribov-Lipatov-Altarelli-Parisi (DGLAP) [43] evolution equations

$$\begin{aligned}
\frac{\partial f_q(x, \mu_F^2)}{\partial \mu_F^2} &= \frac{\alpha_s(\mu_F^2)}{2\pi} \int_x^1 \frac{d\xi}{\xi} \left[P_{qq}\left(\frac{x}{\xi}\right) f_q(\xi, \mu_F^2) + P_{qg}\left(\frac{x}{\xi}\right) g(\xi, \mu_F^2) \right], \\
\frac{\partial g(x, \mu_F^2)}{\partial \mu_F^2} &= \frac{\alpha_s(\mu_F^2)}{2\pi} \int_x^1 \frac{d\xi}{\xi} \left[\sum_q P_{gq}\left(\frac{x}{\xi}\right) f_q(\xi, \mu_F^2) + P_{gg}\left(\frac{x}{\xi}\right) g(\xi, \mu_F^2) \right].
\end{aligned} \tag{2.27}$$

The functions P_{qq}, P_{qg}, P_{gg} and P_{gq} are called the splitting functions, $g(x, \mu_F^2) \equiv f_g(x, \mu_F^2)$ is the gluon density and $f_q(x, \mu_F^2)$ represents the quark or the antiquark density in the hadron, with q spanning all the quark and antiquark flavours. The splitting functions are calculated perturbatively and are illustrated in Fig. 2.9.

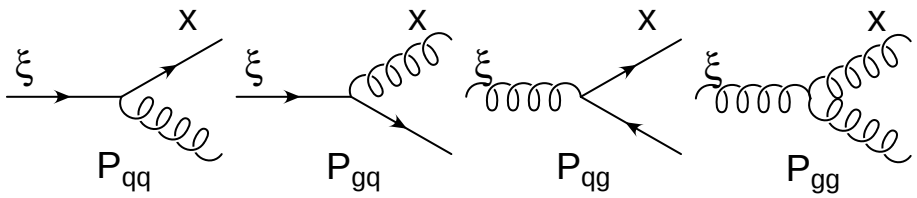

Figure 2.9: The Feynman diagrams corresponding to the DGLAP splitting functions in leading order. A splitting function, for example $P_{gq}(z)$, is interpreted as the probability to find gluon g with momentum fraction z in a quark q.

The DGLAP equations are the analogue of the β function equation (2.20) describing the running of the strong coupling and are among the most important equations in pQCD. In leading logarithmic approximation, the equations realise a resummation of all the leading terms of the type $[\alpha_s \log Q^2]^n$, arising from the dominating diagrams where successive emissions of partons are strongly ordered in transverse momenta (see Fig. 2.10).

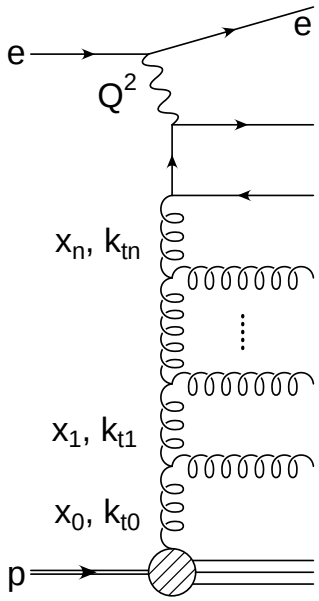

Figure 2.10: Ladder diagram for DIS showing successive emissions of partons. In the region of asymptotically large Q^2, the DGLAP resummation is valid and the dominant contributions are coming from the diagrams where $Q^2 \gg k_{tn}^2 \gg ... \gg k_{t1}^2 \gg k_{t0}^2$. In the region of asymptotically small x, the BFKL resummation is valid, and the dominant diagrams are ordered in x, $x_n \ll ... \ll x_1 \ll x_0$.

The DGLAP equations are expected to become inaccurate for very small values of x ($x \ll 1$), when terms of the type $[\alpha_s \log(1/x)]^n$ become large. The resummation of such terms is described by the Balitsky-Fadin-Kuraev-Lipatov (BFKL) [44] equation, which includes diagrams that are not k_t-ordered.

Through the above resummation techniques one improves the perturbative QCD treatment at very high energies. DGLAP and BFKL include leading contributions (large logarithms) from all higher orders. The need for resummation

can be understood intuitively, since with an increase of energy, the available phase space for emissions becomes larger and the probability for gluon emissions increases, although the coupling is small.

2.3 Non-perturbative QCD

The theory of perturbative QCD presented above provides the basic approach to study hadronic phenomena. The underlying dynamics of collisions of hadrons is described at the parton level, although partons have not been directly observed in nature. The notion of asymptotic freedom provides the explanation why such an approach is viable.

Asymptotic freedom also separates the space-time scale where perturbative theory lives, from the one where the measurements and the experimental setups are made. The perturbative calculations can be trusted on very small scales, of fractions of a femtometer, while the outcome of the process is measured very far away, in detectors. The main observation is that there is no longer a partonic picture, instead hadrons are observed experimentally.

Confinement

The outstanding problem of explaining why quarks and gluons are confined in hadrons still remains to be solved. Confinement can be understood in general terms from the arguments of the running coupling strength α_s, which becomes large for small momentum transfers. This makes the soft interactions very strong and perturbation theory can no longer be applied. However, confinement is not a prediction of perturbative QCD, while asymptotic freedom is. Confinement is a soft phenomenon that must be understood using non-perturbative methods.

There are no generally accepted and uniformly applicable analytical tools to handle the non-perturbative aspects of QCD, starting from first principles. Many non-perturbative methods used to understand these aspects are based on expansions complementary to the ordinary perturbation theory, while others are just phenomenological models inspired from QCD.

One important long space-time ingredient of the parton model is the parton distribution function, giving the structure of hadrons. The non-perturbative x-dependence at small values of Q^2 can only be obtained through parameterizations from experimental data, or from phenomenological models (see for example [42]). For larger values of Q^2, perturbative QCD can be used to evolve these distributions, using the DGLAP equations (2.27).

It is very important to have a description of another long space-time phenomenon, the transition from the stage of quarks and gluons to the stage of hadrons. This phenomenon of hadronization, sometimes called parton fragmentation, can so far only be approached through phenomenological models. Similar to the parton distribution functions, the so called fragmentation functions give the probability for finding a hadron emerging from a high energy quark or gluon.

One can derive evolution equations for fragmentation functions, which are very similar to the DGLAP equations.

There are more aspects to non-perturbative QCD, other than confinement and hadronization. Although not discussed here, these are worth mentioning, for example hadron spectroscopy, chiral symmetry breaking, soft scattering processes. Among the non-perturbative methods used, one can enumerate the lattice QCD (QCD on a discrete space-time lattice), chiral perturbation theory, instanton calculus, $1/N_c$ expansion, etc.

Hadronization

The most outstanding model for the description of hadronization is the Lund string model [45]. In the Lund model the partons are connected by a massless relativistic string, representing an essentially one-dimensional colour flux between them. Due to the self-interaction of gluons, the colour flux lines do not spread in space, but are contained in a thin tube-like region, which can be described approximately by a string. From the available field energy, $q\bar{q}$-pairs will be created, and the system breaks into smaller and smaller pieces until hadrons are formed.

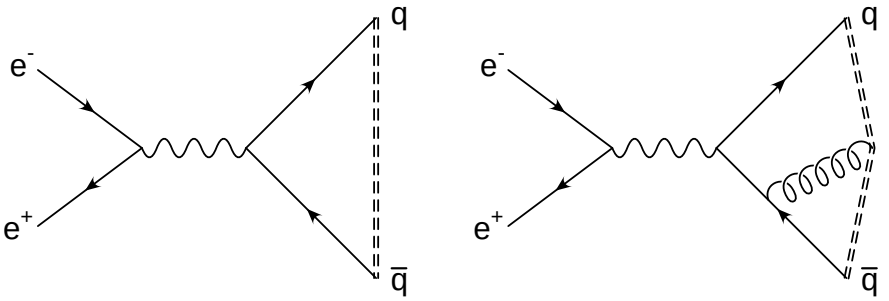

Figure 2.11: In $e^+e^- \to q\bar{q}$, the string (double dashed line) in the Lund model is stretched between a quark and an antiquark; emitted gluons are kinks on the string.

The basics of the string model are best exemplified by considering a string spanned between a quark q and an antiquark $\bar{q}$ as produced in an e^+e^- annihilation (Fig. 2.11a). The colour flux tube goes from the colour triplet charge of the quark to the antitriplet charge of the antiquark. This tube contains a constant amount of field energy stored per unit length. This picture of a linear rising potential between q and $\bar{q}$, and the string formation, is supported by QCD lattice calculations. The string constant κ, representing the energy per unit length of the tube, is known phenomenologically to be $\kappa \approx 1$ GeV/fm.

Within the tube, quark-antiquark pairs can be produced from the field energy. The string breaks into a hadron and a scaled down version of the original string, which can break down through an iterative procedure until the last two hadrons are formed (see Fig. 2.12a). Thus, the procedure is suitable for implementing into Monte Carlo generators, which will be presented in Chapter 3.

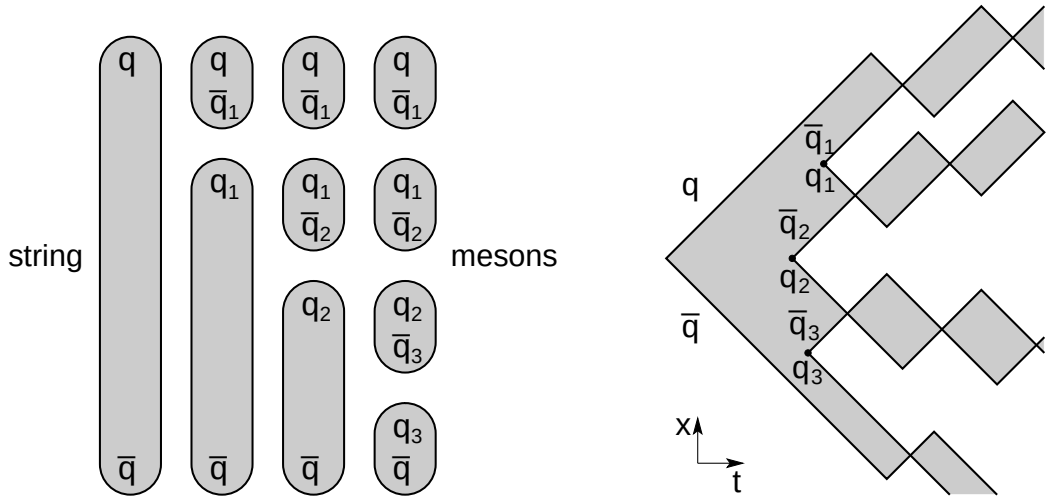

a) b)

Figure 2.12: a) Illustration of the iterative string fragmentation into hadrons. The multiplicity of produced hadrons rises with the available energy of the colour field. b) The dynamics of a $q\bar{q}$ string in the center of mass. The field is broken at different space-time points by the production of quark-antiquark pairs. Hadrons are represented by the 'yo-yo' modes of the massless relativistic string.

The $q\bar{q}$ pairs are produced through a tunneling process, with the production probability proportional to

$$\exp(-\pi m_\perp^2/\kappa) = \exp(-\pi m^2/\kappa) \cdot \exp(-\pi p_\perp^2/\kappa), \tag{2.28}$$

where m is the mass of the produced quark and antiquark and $p_\perp$ represents their transverse momenta (equal in magnitude, but opposite direction) relative to the string. The first factor gives a suppression for production of heavier quarks, and the second one represents a gaussian distribution of the transverse momenta.

The motion of the quark and the antiquark connected via the string is equivalent to a 'yo-yo' mode of the massless relativistic string. In the center of mass frame of the $q\bar{q}$ pair, the quark and antiquark will oscillate back and forth. In order to form a meson, the quark and antiquark which have been produced in two consecutive break-ups, will need to match their energy and momenta to form the meson mass (see Fig. 2.12b).

It is useful to introduce a variable related to the energy and momentum of a particle, namely the rapidity

$$y = \frac{1}{2} \log \left(\frac{E + p_z}{E - p_z} \right), \tag{2.29}$$

where p_z represents the longitudinal component of the particle's momentum. The hadrons produced in the string breaking are distributed evenly in rapidity. They are aligned along the $q\bar{q}$ axis, with transverse momenta provided by their constituent quark-antiquark and longitudinal momenta given by the fragmentation

functions. In every Lorentz frame, the slowest hadrons (small rapidity) will be produced first.

The production of baryons is achieved in a similar way by effectively creating diquark-antidiquark pairs from the field energy, but with a lower probability than the $q\bar{q}$ pairs, resulting in a suppression of baryon production.

The fragmentation of gluons is solved elegantly by considering gluons as localized excitations ('kinks') on the massless relativistic string. Thus, the motion of the string stretched between quarks gets a kick (Fig. 2.11b), and the fragmentation is done in the same way. The procedure can be generalized to many gluons. This scheme is infrared stable, as all soft and hard gluons correspond to kinks on the string, and a smooth transition between soft and hard emitted gluons is achieved.

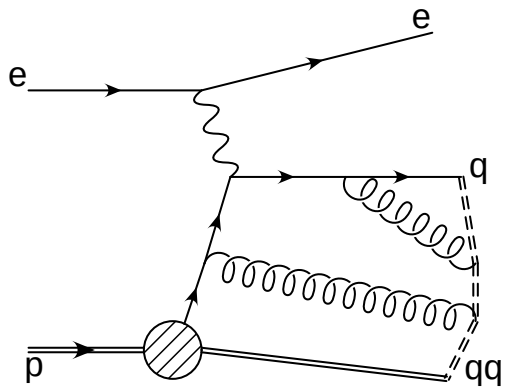

Figure 2.13: The Lund string model applied to deep inelastic electron-proton scattering.

In the case of DIS and hadronic collisions, the initial state colour charges and the hadron remnant(s) have to be taken into account when considering the fragmentation (see Fig. 2.13). Depending on the parton which takes part in the hard interaction, the hadron remnant is modelled in such a way as to preserve the correct quantum numbers of the hadron. If the interacting parton is a valence quark, the remnant is represented by a diquark, and if it is a gluon, the remnant is modelled as a quark and a diquark. The longitudinal and transverse momenta of the partons in the remnant are given by phenomenological models.

In high energy processes with many quarks and gluons the way these are connected via the confining colour field is important for the way the final state hadrons are produced. The field topology must be taken into account, since the position of the colour charges is not enough to define the confining field. Conventionally, in the Lund model, the colour topology of the fields is given by the perturbative phase. In perturbative QCD it is possible to compute amplitudes for different colour combinations of the quarks and gluons, which can be associated to different configurations for the colour fields. The strings will be stretched between colour charges in such a way to conserve the colour flow from the perturbatively calculated amplitudes.

Chapter 3

Hard and soft interplay

The principle of factorization underlies all theoretical calculations of high energy processes involving hadrons and represents the field theory realization of the parton model. Simply expressed, factorization is a statement that short and long distance contributions to the physics processes can be separated. The predictive power comes from the fact that the incalculable long distance effects are universal, and can be extracted in one process and used in another. Proving factorization represents a great success of QCD [46].

It is, however, difficult to approach analytically the study of the interplay between the short distance processes, called hard, and the long distance ones, called soft. While perturbative QCD is successful in describing the hard processes, one has to rely on phenomenological models to gain understanding about the soft physics. Furthermore, phenomenological models make the connection between theoretical expectations and the experimental data. The models are able to transform the theoretical predictions into the experimentally observed hadronic final states.

3.1 Monte Carlo event generators

Monte Carlo event generators are complete models for high energy scattering, situated at the border between theory and experiment. They comprise the essential elements of perturbative QCD and Electro-Weak (EW) interactions, as well as phenomenological models describing the soft processes. Their basis is the fact that the differential cross section is a probability distribution in the kinematic variables, and Monte Carlo methods can be used to generate phase-space points according to this distribution. Scattering events can be generated this way, and the hadronic final state can be directly compared to the experiment.

The main philosophy behind the Monte Carlo generators is the factorization of the physics process into different phases which can be treated separately. These phases are similar for a deep inelastic scattering Monte Carlo (for example LEPTO [47]) or a generator which describes hadron-hadron collisions (like PYTHIA [48]), and are summarized in Fig. 3.1.

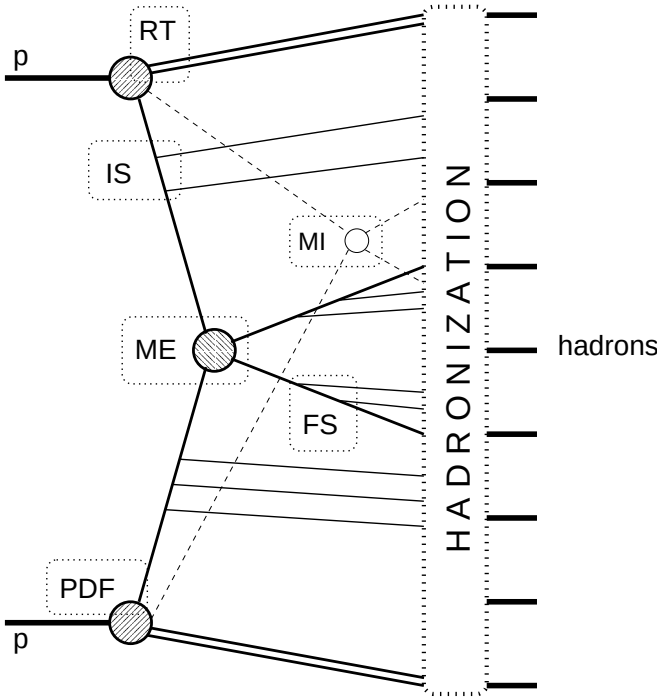

Figure 3.1: The structure of a Monte Carlo event generator, exemplified with a hadron-hadron collision:

1. The incoming particles coming towards each other have partonic substructures, described by parton distribution functions (PDF) giving the flavour and energy sharing of the interacting partons.
2. Through series of branchings, initial parton showers (IS) will evolve the partons in pQCD using the DGLAP equations (2.27), up to the scale of the hard interaction.
3. The hard interaction between the two partons gives the main characteristics of the event, and is described by matrix elements (ME) calculable in perturbation theory.
4. The outgoing quarks and gluons undergo final state parton showering (FS), based on perturbative evolution equations for fragmentation functions as described by DGLAP equations.
5. Additional interactions may occur between the partons in the incoming hadrons, as they overlap. These multiple interactions (MI) are semi-hard.
6. The partons entering the hard interactions leave behind hadron remnants. The internal structure of the remnant is modelled in what is called remnant treatment (RT).
7. The hadronization step will connect the colour charged objects (quarks, gluons and remnants) by force fields. Additional soft interactions can occur before these fields (*e.g.* strings) will fragment into colour neutral hadrons.
8. Many produced hadrons are unstable and will decay.

The interplay between hard and soft physics offers the opportunity to learn more about non-perturbative aspects of QCD, using the tools provided by perturbative QCD. In the following, several methods and phenomenological models used in this thesis will be described.

3.2 Soft Colour Interactions

The soft colour interaction models were developed with the aim of understanding better the non-perturbative dynamics and to provide a unified description of all final states. The basic assumption is that variations in the topology of the confining colour force fields (strings) can lead to different hadronic final states after hadronization.

There are two phenomenological models using this assumption, the soft colour interaction (SCI) model [49] and the generalized area law (GAL) model [50]. These are added to Monte Carlo generators (LEPTO and PYTHIA) which simulate the interaction dynamics of ep and $p\bar{p}$ scattering, and provide a complete final state of observable particles. This gives powerful tools for detailed investigations of the models and their ability to reproduce experimental data.

The starting point is that the hadronic final state is produced through the hadronization of partons emerging from a hard scattering process which can be well described by perturbative QCD. The basic new idea is that there may be additional soft interactions at a scale below the perturbative treatment. These soft colour interactions do not change the dynamics of the hard scattering, but change the colour topology of the state such that another hadronic final state may emerge after hadronization. The colour topology is changed via a soft exchange of colour-anticolour representing non-perturbative gluon exchange.

The soft colour interaction (SCI) model is formulated in a parton basis, where colour exchanges are done between the partons emerging from the hard scattering process (including remnants of initial hadrons). This can be viewed as the perturbatively produced quarks and gluons interacting softly with the colour medium of the hadron as they propagate through it. This should be a natural part of the process in which bare perturbative partons are dressed into non-perturbative ones and colour flux tubes are formed between them.

The probability for a soft exchange to occur is described by a phenomenological parameter P, which is the only parameter of the model. The number of soft exchanges will vary from event to event and can change the colour topology such that, in some cases, colour singlet subsystems arise, as illustrated in Fig. 3.2. In the figure, a colour exchange between the perturbatively produced gluon and the quark in the remnant has taken place. This type of exchanges are of particular importance for the so called rapidity gap events (having a region in rapidity without particles).

The generalized area law (GAL) model is formulated in a string basis, since strings are assumed in this model to be the proper states for soft exchanges that may not resolve partons. This model is very similar in spirit to the SCI model.

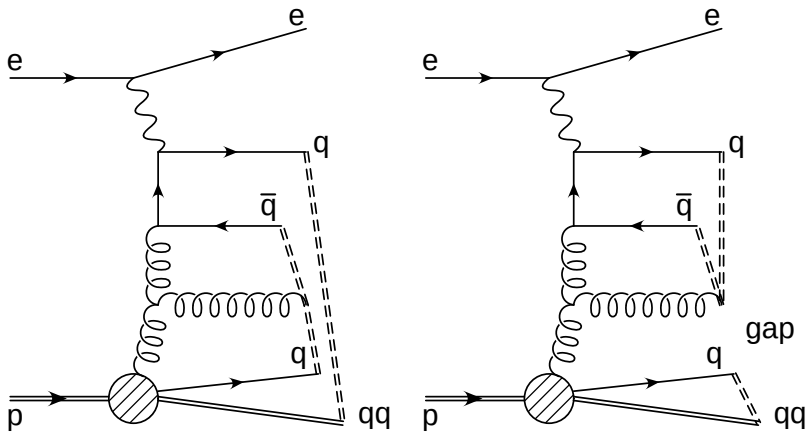

Figure 3.2: Photon-gluon fusion in deep inelastic scattering with a string configuration in a) the conventional Lund string model and b) after a soft colour exchange between the remnant and the hard scattering system.

Instead of soft exchanges between partons, the GAL model assumes that soft colour exchanges between strings can change the colour topology, resulting in another string configuration, as can also be represented by Fig. 3.2.

The probability for two strings to interact is in the GAL model obtained as a generalization of the area law suppression e^{-bA} with the area A swept out by a string in energy-momentum space. The model uses the measure $A_{ij} = (p_i + p_j)^2 - (m_i + m_j)^2$ for the piece of string between two partons i and j. This results in the probability $P = P_0[1 - \exp(-b\Delta A)]$ depending on the change ΔA of the areas spanned by the strings in the two alternative configurations of the strings, *i.e.* , with or without the topology-changing soft colour exchange. The exponential factor favours making 'shorter' strings, *e.g.* , events with gaps, whereas making 'longer' strings is suppressed. The fixed probability for soft colour exchange in SCI is thus in GAL replaced by a dynamically varying one.

Since the soft processes cannot alter the hard perturbative scattering processes, the latter is kept unchanged in the models. Therefore, the hard parton level interactions are treated using standard scattering matrix elements, plus initial and final state parton showers (see Fig. 3.1). Thus, the set of quarks and gluons, including those in the hadron remnants, are generated as in conventional Monte Carlo generators describing ep or $p\bar{p}$ hard scattering processes. The SCI and GAL models are then added as an extra intermediate step before the hadronization is performed (step 7 in Fig. 3.1).

These models, therefore, employ perturbative QCD on the parton level as a firm basis to approach the soft dynamics, which is the major unsolved problem in QCD.

3.3 Saturation Model

The partonic picture presented before provides the basis for introducing the parton distribution functions and the key concept of factorization. The process of deep inelastic scattering is viewed in the infinite momentum frame, where the content of a proton is probed by a virtual photon (virtuality given by Q^2). The partons are manifest in this frame, and the virtual photon makes a localized ($\Delta x \sim 1/Q$) and instantaneous ($\Delta t \sim 1/Q$) measurement of the quark and gluon structure of the proton.

An alternative view of DIS can be obtained in the proton rest frame. In this frame, the interaction distance and time get strongly Lorentz transformed, to values much larger than the proton size. The interaction looks like a fluctuation of the virtual photon into quark, antiquark and gluons which happens before the photon reaches the target (see Fig. 3.3).

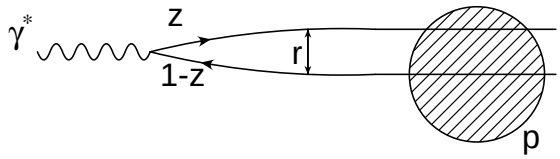

Figure 3.3: Illustration in the proton rest frame of the fluctuation of the virtual photon into a $q\bar{q}$ dipole upstream from the proton.

The deep inelastic scattering of a virtual photon on a proton can now be viewed as being factorized into three stages: 1) the virtual photon fluctuates into a colour dipole state built of a quark and an antiquark, 2) interaction of this state with the static proton, and 3) formation of the hadronic final state. In this dipole picture, the cross section is given by the following formula

$$\sigma^{\gamma^* p} \;=\; \int_0^1 dz \int d^2r \; |\Psi(z,r)|^2 \, \hat{\sigma}(x, r^2), \tag{3.1}$$

where r denotes the transverse separation between q and $\bar{q}$ in the colour dipole, z is the longitudinal momentum fraction of the quark in the photon (correspondingly $1-z$ for the antiquark) and x is the Bjorken parameter, i.e. $x = Q^2/(2pq)$. The cross-section $\hat{\sigma}(x, r^2)$ is the dipole–proton total cross-section, and $\Psi(z, r)$ denotes the wave function of the photon to produce a dipole.

The photon virtuality introduces the scale $1/Q$ for the transverse dimension of the $q\bar{q}$ pair. For small transverse sizes ($r < 1/Q$) of the fluctuating state, the dominant scattered state is the $q\bar{q}$ colour dipole. The scattering of such a small dipole can be calculated in perturbative QCD, and the cross section is related to the gluon density of the target. The total cross section has a simple scaling behaviour, so called colour transparency, $\sigma^{\gamma^* p} \sim 1/Q^2$ (modulo $\log Q^2$), combined with a powerlike dependence in x as typically observed in DIS.

Dipoles of large size ($r > 1/Q$) will interact with much larger cross section due to the increased gluon content of the dipole. Because of the large colour

separation of the dipole, the perturbative calculation of the photon wave function is no longer appropriate. The incorporation of the unitarity constraint for high energy scattering may be realised by assuming that the cross section has the saturation property $\sigma^{\gamma^* p} \to const.$

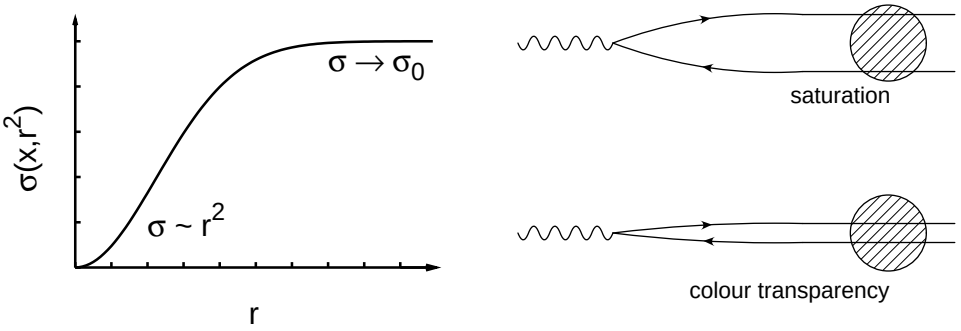

Figure 3.4: The dipole-proton cross section and the two regimes of colour transparency and saturation.

The saturation model introduced by Golec-Biernat and Wüsthoff (GBW) [51] attempts to describe both properties in a common framework. Through an economic parameterization of the dipole-proton cross section

$$\hat{\sigma}(x, r^2) \;=\; \sigma_0 \left[1 - \exp\left(-\frac{r^2}{4R_0^2(x)} \right) \right], \tag{3.2}$$

the perturbative regime, of a single hard scattering, is unified with the soft regime, when multiple scatterings occur (see Fig. 3.4). The saturation radius $R_0(x)$, which controls the transition between the two regimes, is given by the following x dependence

$$R_0(x) \;=\; \frac{1}{Q_0} \left(\frac{x}{x_0} \right)^{\lambda/2}, \tag{3.3}$$

where $Q_0 = 1$ GeV. The three parameters of the model σ_0, λ and x_0, have been fitted to describe experimental DIS data for small values of x.

The central concept is the x dependence of the saturation radius, which introduces a new kind of saturation, called small-x saturation. While x decreases, one has to go to smaller distances (higher Q^2) in order to resolve the dense parton structure of the proton. Thus, $R_0^2(x) = 1/Q^2$ defines a critical line, separating the regime of a single gluon exchange from the multiple gluon exchange.

In this way, the dipole-proton cross section will exhibit the colour transparency when the dipole is small, *i.e.* $\hat{\sigma}(x, r^2) \sim r^2$, as well as the saturation property when the dipole is large $\hat{\sigma}(x, r^2) \sim \sigma_0$, allowing the study of the interplay between the two regimes.

3.4 Gluon virtuality and k_t factorization

In the QCD parton model presented so far, the cross sections for hadronic interactions were written in terms of a process-dependent hard matrix element convoluted with universal parton density functions, the scaling violations of which are described by the DGLAP evolution. Because of the strong ordering of virtuality in the DGLAP evolution, the virtualities of the parton entering the hard interaction could be neglected compared with the large scale Q^2 of the probe. In this approximation the initial partons are treated as collinear with the incoming hadron and the cross section is obtained in the collinear factorization scheme as

$$\sigma^{cf} = \sum_i \int_0^1 dx\, \hat{\sigma}_i(x) f_i(x, \mu^2) \ . \tag{3.4}$$

When the longitudinal momentum fraction x of the partons becomes smaller, there are no longer grounds for neglecting their transverse momenta k_t. Attempts have been made in models to incorporate the transverse momenta by a random shift according to simple distributions. Although these models are lacking theoretical foundation, they showed the effect and importance of gluon transverse momenta.

It is believed that the theoretically better approximation of the small-x domain is given by the BFKL evolution. Here large logarithms $\alpha_s \log(1/x)$ are resummed to all orders, in a procedure where the transverse momenta of the propagating partons are considered and their virtuality is not ordered. Another evolution equation which resums these type of logarithms is the Ciafaloni-Catani-Fiorani-Marchesini (CCFM) [52] evolution equation. This evolution introduces angular ordering of the emission of the partons, in order to include correctly gluon coherence effects. In the limit of small x it is equivalent to BFKL, but it is also similar to the DGLAP evolution for large x and high Q^2.

In both frameworks, it is possible to factorize the cross section just as for DGLAP, as a convolution of hard matrix elements with universal parton distributions. The convolution is done also over the transverse momentum k_t, and one talks about k_t factorization [53] or semihard approach [54]. The cross section for a physical process is given by

$$\sigma^{kf} = \sum_i \int_0^1 dx \int d^2k_t\, \hat{\sigma}_i(x, k_t^2)\, \mathcal{F}_i(x, k_t^2, \mu^2) \ , \tag{3.5}$$

where $\hat{\sigma}_i(x, k_t^2)$ is an off-shell (transverse momentum dependent) partonic cross section, and $\mathcal{F}_i(x, k_t^2, \mu^2)$ are the so called unintegrated parton density functions.

The off-shell partonic cross sections are calculated based on Feynman diagrams, where the virtualities and possible polarization of the incident partons are taken into account. The off-shell matrix elements have a rather complicated structure and are known for several processes, including heavy quark production [53] in leading order (LO). At this order they already include some part of

the next-to-leading order (NLO) corrections of the collinear approach. In k_t factorization, the transverse momenta of the incoming gluons are only restricted by kinematics and the gluons acquire a virtuality similar to the internal propagators in a complete fixed order calculation (see Fig. 3.5).

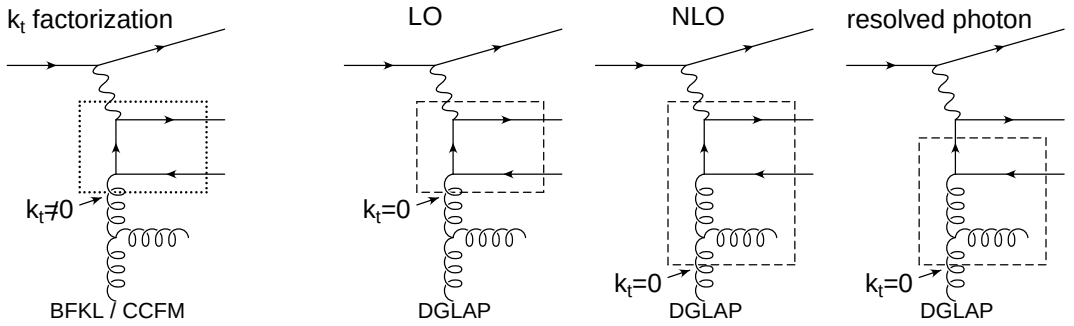

Figure 3.5: Representation of the photon-gluon fusion in the k_t factorization approach, compared to the fixed order LO, NLO and resolved photon processes in the collinear approach.

The unintegrated parton density functions $\mathcal{F}_i(x, k_t^2, \mu^2)$ determine the probability to find a parton carrying the longitudinal momentum fraction x and the transverse momentum k_t in the hadron at the factorization scale μ. They are described by the BFKL or the CCFM evolution equations and reduce to the conventional parton densities once the k_t dependence is integrated out, *i.e.*

$$f_i(x, \mu^2) \simeq \int_0^{\mu^2} dk_t^2 \; \mathcal{F}_i(x, k_t^2, \mu^2). \tag{3.6}$$

The approximate sign indicates that there is no strict equality, as neither parton distributions are observable. The dependence on the scale μ^2 is not present in the unintegrated densities obeying the BFKL equation, while in the case of CCFM it is present and represents the maximum angle allowed for gluon emissions.

In the non-perturbative region, for low values of transverse momentum k_t, the unintegrated parton densities no longer obey the perturbative evolution equations, and one needs to rely on models and parameterizations that can be obtained from the collinear parton densities $f_i(x, \mu^2)$.

By explicitly carrying out the integration over k_t in Eq. (3.5), one can obtain a form fully consistent with the collinear factorization (3.4), where the coefficient functions $\hat{\sigma}_i(x)$ are no longer evaluated in fixed order perturbation theory, but supplemented with resummation of all $\alpha_s \log(1/x)$ contributions for small x.

Thus, the specific effects of parton virtualities become manifest – one obtains additional contributions to the cross section due to the integration over the k_t region above μ, or broadening of the transverse momenta of produced hadrons due to the extra transverse momentum of the interacting partons.

Chapter 4

BRST quantization

Gauge symmetries are quintessential for quantum field theories describing the known fundamental interactions of nature. The interactions between matter particles arise by imposing the requirement of local gauge invariance of the theory containing these particles. The presence of the symmetry indicates, however, that the theory is formulated in a redundant way, with local degrees of freedom that do not enter the dynamics. Although these can in principle be eliminated, there are reasons for not doing so, like covariance, locality of interaction or simplified calculations.

The quantization of gauge theories is not always straightforward and it involves a gauge fixing procedure to render dynamical the degrees of freedom. Also, ghost fields are introduced to compensate for the effects of the gauge degrees of freedom, so that unitarity is preserved. It has been realised by Becchi-Rouet-Stora and Tyutin (BRST) [55], that the gauge-fixed theory retains a global symmetry involving transformations of both the fields and the ghosts. This BRST symmetry is what remains of the original gauge invariance.

The BRST transformations critically involve the ghost fields, which are useful for the quantization of gauge field theories. It is desirable to have a formulation of gauge theories that automatically incorporates the BRST symmetry and includes the ghosts from the onset. The so called *antifield BRST formalism* [56] relies on the BRST symmetry as a fundamental principle and provides a powerful tool for quantization and renormalization of gauge theories.

The BRST formalism has the advantage of quantizing theories which cannot be treated by the Faddeev-Popov [13] functional integral approach, for instance supergravity. It also has broader applications, being used to restate and simplify proofs of theorems in renormalization theory [57]. The BRST formalism has also been stimulated by the development of string theory. It gained popularity when the open bosonic string field theory was successfully quantized, and it proved to be useful for closed string theory and for topological field theories. Extensive reviews about BRST symmetries and the antifield formalism can be found in [58] and [59].

4.1 Quantization of Yang-Mills

In the following, a short account of the antifield BRST formalism will be presented, illustrated on the non-abelian Yang-Mills theory [12]. This will lead in the end to the quantization of Yang-Mills theories, and subsequently to the quantization of QCD as presented in Chapter 2.

The starting point is represented by the Yang-Mills action, which is a functional of the fundamental fields $A^a_\mu(x)$ and is written in terms of the field strength $F^a_{\mu\nu}$ (defined by Eq. 2.4)

$$S_0[A^a_\mu] = -\frac{1}{4}\int d^4x F^a_{\mu\nu}F^{\mu\nu}{}_a. \tag{4.1}$$

The action is invariant under the local gauge transformations (2.7), which can be written in infinitesimal form

$$\delta A^a_\mu = \partial_\mu \epsilon^a(x) + g f^a{}_{bc}\epsilon^b(x)A^c_\mu(x) = D_\mu{}^a{}_b\epsilon^b(x), \tag{4.2}$$

where $D_\mu{}^a{}_b$ is the covariant derivative from Eq. (2.3) written in the adjoint representation. In general, these are called generators of the gauge transformations and are functions of the fields of the theory, while the functions $\epsilon^a(x)$ are called gauge parameters.

The first step in the antifield BRST formalism is to enlarge the original configuration space consisting of the fields $A^a_\mu(x)$, to include additional fields like ghost fields and antifields. Corresponding to the number of gauge invariances at the classical level ($a = 1 \dots N_c^2 - 1$ in Eq. 4.2), the same number of ghosts are needed at the quantum level. In order to build the BRST symmetry, it is useful to introduce the ghosts at the classical stage, so $N_c^2 - 1$ fields denoted $\eta^a(x)$ will be added.

The whole set of fields is now $\phi^i \equiv \{A^{\mu a}, \eta^a\}$ and a new conserved charge, called ghost number, is assigned to these fields. The original fields $A^{\mu a}$ have ghost number zero, whereas the ghosts have ghost number one. The ghosts have opposite statistics to the corresponding gauge parameters $\epsilon^a(x)$, so η^a are fermions.

Next, for each field ϕ^i one introduces an antifield $\phi^*_i \equiv \{A^*_{\mu a}, \eta^*_a\}$. The statistics of each field ϕ^*_i is opposite to that of the corresponding ϕ^i (see Fig. 4.1). Although at this stage the antifields are introduced as a tool to develop the formalism, they can be interpreted as the 'sources' of the BRST transformations. These fields will be eliminated by a gauge fixing procedure, and will not influence calculations of observables.

The second step is to introduce in the space of fields and antifields a structure called the antibracket

$$(X, Y) \equiv \frac{\partial^R X}{\partial \phi^i}\frac{\partial^L Y}{\partial \phi^*_i} - \frac{\partial^R X}{\partial \phi^*_i}\frac{\partial^L Y}{\partial \phi^i}\,, \tag{4.3}$$

for any two functionals X and Y of the fields and antifields. The antibracket is antisymmetric, it carries ghost number one and has odd statistics. The antibracket

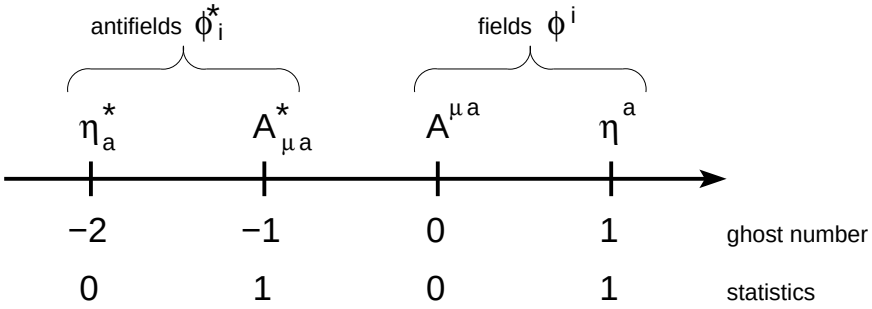

Figure 4.1: Properties of the minimal sector of fields and antifields in the antifield BRST formalism for Yang-Mills theory (statistics: 0=bosons, 1=fermions).

is similar to the Poisson bracket used at a classical level in the Hamiltonian formalism, but it corresponds to the Lagrangian formalism at the classical or quantum level. The antifields ϕ^*_i can be thought of as conjugate variables to the fields ϕ^i, since $(\phi^i, \phi^*_j) = \delta^i_j$.

In the next step, the classical action S_0 is extended to include terms involving ghosts and antifields. Let $S[\phi^i, \phi^*_i]$ be an arbitrary functional of the fields and antifields, with the same dimension as the action S_0, ghost number zero and even statistics. The equation

$$(S, S) = 0\,, \tag{4.4}$$

is called the *master equation*, and is the fundamental equation of the BRST formalism. The solution to this equation represents the starting action to quantize covariantly the gauge theory, and if the equation is solved the BRST symmetry will be completely determined.

To make contact with the original theory, the solution to the master equation must contain the original action S_0. The boundary condition

$$S[\phi^i, \phi^*_i]\big|_{\phi^*_i=0} = S_0[A^a_\mu]\,, \tag{4.5}$$

ensures the correct classical limit, when the antifields are trivially eliminated. The solution can be found by expanding S into a power series of the antifields, and the first term is necessarily S_0. For the case of Yang-Mills, the first terms of this expansion are given by

$$S = \int d^4x \left\{ -\frac{1}{4} F^a_{\mu\nu} F^{\mu\nu}{}_a + A^*_{\mu a} D^{\mu a}{}_b \eta^b + \frac{1}{2} \eta^*_a f^a{}_{bc} \eta^b \eta^c \right\}. \tag{4.6}$$

In the first order, the contributions are driven by the gauge generators $D^{\mu a}{}_b$ and the structure constants $f^a{}_{bc}$ of the gauge algebra.

The BRST symmetry can now be constructed with the help of the functional S. The antifield formalism exhibits BRST symmetry even before gauge-fixing. After gauge fixing, this symmetry will survive and can be regarded as the substitute of the original gauge invariance. The BRST transformation of a

functional X is defined via the antibracket and the solution of the master equation

$$sX \equiv (X, S) \tag{4.7}$$

The BRST operator s has the property of nilpotency, $s^2X = 0$, which follows from the properties of the antibracket. The field-antifield action S is BRST symmetric, since $sS = 0$ via the master equation. The same is true for any observable $\mathcal{O}$ of the theory, *i.e.* $s\mathcal{O} = 0$.

It is instructive to look at the BRST transformation rules for the fields (which can be determined from Eq. 4.7)

$$sA^{\mu a} = D^{\mu a}{}_b \eta^b \,, \quad s\eta^a = \tfrac{1}{2} f^a{}_{bc} \eta^b \eta^c \,, \tag{4.8}$$

since the BRST transformation of the gauge fields $A^{\mu a}$ is similar to their gauge transformations (4.2), where the role of the gauge parameters ϵ^a is now taken by the ghost fields η^a.

The next process towards the quantization of the theory, is the process of gauge-fixing. Although ghosts have been incorporated, the action S still possesses gauge invariance and is not yet suitable for quantizing via the path integral approach. A gauge-fixing is needed and one introduces the concept of gauge-fixing fermion Ψ, which is a functional of only the fields, with odd statistics and ghost number -1.

Since there is no field with negative ghost number in the minimal sector of fields (see Fig. 4.1), one needs to introduce additional fields, called auxiliary fields, to construct the fermion Ψ. These are trivial pairs of fields $\{\bar{\eta}_a, B^a\}$, where $\bar{\eta}_a$ has ghost number -1 and are known as Faddeev-Popov antighosts of η^a. These fields have corresponding antifields $\{\bar{\eta}^{*a}, B^*_a\}$ constructed in the same way as presented before.

In the configuration space containing all the fields $\phi^i \equiv \{A^{\mu a}, \eta^a, \bar{\eta}_a, B^a\}$ and antifields $\phi^*_i \equiv \{A^*_{\mu a}, \eta^*_a, \bar{\eta}^{*a}, B^*_a\}$, the solution to the master equation is extended to contain the new fields, by

$$S \to S + \int d^4x \, \bar{\eta}^{*a} B_a. \tag{4.9}$$

This solution is called non-minimal action and shares all the properties of the minimal action from Eq. (4.6), including the BRST symmetry.

The gauge-fixing fermion Ψ can be chosen freely and it corresponds to the choice of the gauge-fixing procedure. Choosing a particular Ψ, however, can greatly simplify calculations of observables. Also, one would like to eliminate all the antifields from the theory before computing observables. The antifields cannot be simply set to zero, since the action S would reduce to the classical action S_0 which is not suitable for quantization. The elimination of the antifields from the action and incorporation of the gauge fixing is done via

$$\phi^*_i = \frac{\partial \Psi}{\partial \phi^i} \,. \tag{4.10}$$

The gauge-fixed action obtained in this way

$$S_\Psi \equiv S\left[\phi^i, \phi_i^* = \frac{\partial \Psi}{\partial \phi^i}\right], \tag{4.11}$$

will retain the global BRST symmetry as a remnant of the original gauge invariance.

To obtain the covariant gauge in Yang-Mills theories, the following gauge-fixing can be chosen

$$\Psi = \int d^4x\ \bar{\eta}_a \left(-\frac{\xi}{2} B^a + \partial^\mu A^a_\mu\right). \tag{4.12}$$

Eliminating all the antifields using Eq. (4.10) leads to the gauge-fixed action

$$S_\Psi = \int d^4x \left\{-\frac{1}{4} F^a_{\mu\nu} F^{\mu\nu}{}_a + \partial_\mu \bar{\eta}_a D^{\mu a}{}_b \eta^b - \left(\frac{\xi}{2} B_a - \partial^\mu A_{\mu a}\right) B^a\right\}. \tag{4.13}$$

The final step is to construct the path integral corresponding to the gauge-fixed action S_Ψ, and to perform the gaussian integral over the fields B^a, obtaining

$$Z = \int \mathcal{D}A^a_\mu \mathcal{D}\eta_a \mathcal{D}\bar{\eta}_a \exp\left(i \int d^4x \left\{-\frac{1}{4} F^a_{\mu\nu} F^{\mu\nu}{}_a + \partial_\mu \bar{\eta}_a D^{\mu a}{}_b \eta^b - \frac{1}{2\xi} (\partial^\mu A^a_\mu)^2\right\}\right) \tag{4.14}$$

The action from the path integral (4.14) has BRST symmetry and is invariant under the transformations of the fields and ghosts from Eq. (4.8), supplemented with the BRST transformation of the antighosts,

$$s\bar{\eta}^a = \frac{1}{\xi} \partial^\mu A^a_\mu \,. \tag{4.15}$$

These are the global symmetries left at the quantum level from the original classical gauge symmetries.

Starting with the properly defined path integral Z one can perform perturbation theory and calculate propagators of the Yang-Mills theory. The introduction of quarks in the theory will lead to QCD, which can be quantized in the same manner. Through the specific choice of the gauge-fixing fermion from (4.12), in the BRST formalism one can obtain the same functional integral (2.15) as in the Faddeev-Popov procedure.

Chapter 5

Summary of papers

5.1 Diffractive hard scattering

Diffraction is an old subject which goes back into pre-QCD times, when hadronic interactions were described using the Regge approach. The interactions where one of the participating hadrons will get 'diffracted' off the other hadron which remains intact were always considered soft, thus suitable for Regge phenomenology. In the modern QCD times, the idea of understanding diffraction on the parton level, gave birth to a new branch of *diffractive hard scattering*. The introduction of a hard scale would give the possibility of resolving partons and making perturbative QCD calculations.

The field of diffractive hard scattering was born with the proposal by Ingelman and Schlein [60], that one should use a hard scattering process in connection with a diffractive event, to investigate the structure of the 'pomeron', an exchanged object with zero quantum numbers believed to mediate the diffractive scattering. This was followed later on by the experimental discovery at CERN [61], when striking events were observed in $p\bar{p}$ collisions, having jets of hadrons with a high transverse momentum (the signature of a hard scattering) and a leading proton carrying a large fraction $x_F \gtrsim 0.9$ of the beam proton momentum (the definition of diffraction).

The requirement of having an intact proton after the scattering, taking a large fraction of the beam momentum can be translated through kinematical constraints into a rapidity gap. A rapidity gap simply represents a region in rapidity with no produced particles. Instead of the rapidity y, it is convenient to use the *pseudorapidity* $\eta = -\log\tan\theta/2 \approx y$, since it is written in terms of the polar angle θ with respect to the z axis of the beam (the approximation becomes exact for massless particles). The requirement of a large rapidity gap adjacent to the proton, which experimentally means a region in the detector with no particles, is an alternative definition of diffraction.

Although predicted and proposed [60] as being a cleaner process for investigating the partonic structure of the pomeron, the observation of diffractive deep inelastic scattering events at HERA [62] came as a surprise. The observation of a high fraction ($\sim 10\%$) of rapidity gaps events in DIS is well explained in terms

of the pomeron model. It was soon shown, however, that this model fails to reproduce the hard diffractive data ($\sim 1\%$ of events have gaps) at the $p\bar{p}$ collider at the Tevatron, when parameterizations of the pomeron structure functions and pomeron flux from HERA were used.

In diffractive hard scattering, the rapidity gap in the forward or backward rapidity region connects to the soft part of the event and non-perturbative effects on a long space-time scale are important. This is the philosophy behind the soft colour interaction models, which provide a different approach to diffraction.

Both models, SCI and GAL, give a good description of diffractive DIS events at HERA, where the only parameter of each model has been fitted. They also give good results when applied to $p\bar{p}$ collisions at the Tevatron, as described in the papers below (Papers I – VI).

It should be noted that non-diffractive observables are described as well by the soft colour interaction models, for example the observed rate of high-$p_\perp$ charmonium and bottomonium at the Tevatron [63], which is factors of ten larger than the predictions based on conventional pQCD.

A different kind of rapidity gap events have been observed in $p\bar{p}$ collisions at the Tevatron [64], with a central rapidity gap between two high-$p_\perp$ jets. This gap corresponds to a large momentum transfer across the gap, and it cannot be described satisfactory by soft processes, but needs to be explained in terms of a hard colour singlet exchange [65].

Paper I

This paper compares the results of the soft colour interaction models with the recent experimental data from the $p\bar{p}$ collisions at the Tevatron [66], on high $p_\perp$ dijet events with an observed leading antiproton which signals diffraction. Both the SCI and GAL models are able to reproduce the fraction of observed diffractive events without introducing any new parameters, and keeping the only parameter fixed at its fitted value from diffractive DIS. The models give a good agreement with the kinematical distributions (transverse momentum and rapidity of the jets) for this type of event.

Other models cannot reproduce the measured diffractive ratio, the Monte Carlo generator Pythia alone gives too small rates, and the standard pomeron model gives larger cross section for diffractive events.

The measurement of the leading antiproton provides a test of how exactly the beam particle remnant is handled in the models. Several alternatives for treating the remnant have been investigated, resulting in substantial variations that show some model uncertainties.

Paper II

This paper presents a very detailed study of the soft colour interaction models applied to $p\bar{p}$ collisions, considering also the general problem of the underlying

Table 5.1: Ratios diffractive/inclusive for hard scattering processes in $p\bar{p}$ collisions at the Tevatron, showing experimental results from CDF and DØ collaborations compared to the SCI and GAL soft colour exchange models.

Observable	$\sqrt{s}$		Ratio [%]		
	[GeV]	Experiment	Observed	SCI	GAL
W + gap	1800	CDF	1.15 ± 0.55	1.2	0.8
Z + gap [a]	1800	DØ	$1.44\ ^{+\ 0.62}_{-\ 0.54}$	1.0	0.5
$b\bar{b}$ + gap	1800	CDF	0.62 ± 0.25	0.7	1.4
J/ψ + gap [a]	1800	CDF	1.45 ± 0.25	1.4	1.7
$jets$ + gap	1800	CDF	0.75 ± 0.10	0.7	0.6
$jets$ + gap	1800	DØ	0.65 ± 0.04	0.7	0.6
$jets$ + gap	630	DØ	1.19 ± 0.08	0.9	1.2
gap + $jets$ +gap [b]	1800	CDF	0.26 ± 0.06	0.2	0.1
$\bar{p}$ + $jets$ + gap [b]	1800	CDF	0.80 ± 0.26	0.5	0.4

[a] Predictions which have been confirmed later on

[b] Ratio of two-gap events to one-gap events

event including the beam particle remnants. All available hard diffractive data from the $p\bar{p}$ collisions at the Tevatron are reviewed in this paper (see Table 5.1), and compared with the results from the SCI and GAL models which were tuned to diffractive DIS data.

A good description is found for production of W, beauty and jets in diffractive events defined by a rapidity gap in the forward region. Also the rates of jet events with a leading antiproton, or in association with two rapidity gaps in the forward and backward region, are well described.

Of special importance are the diffractive events with both a leading proton and a leading antiproton with associated gaps. These events occur naturally in the soft colour interaction models, where the final colour string topology may produce two rapidity gaps in the same event through a single mechanism. The observed events at the Tevatron [67], with a dijet system in the central rapidity region and gaps or leading particles in the forward/backward direction, are well described.

Predictions for diffractive Z and J/ψ production are given. The latter is particularly interesting, since the soft exchange mechanism produces both a gap and a colour singlet $c\bar{c}$ state in the same event.

The soft colour interaction approach is also compared with the pomeron based models for diffraction and possibilities to experimentally discriminate between these different approaches are discussed.

Paper III

This paper summarizes the success of the SCI and GAL models in describing hard diffractive scattering at the Tevatron. The early prediction for production of J/ψ in association with rapidity gaps was found to be correct (see Table 5.1).

Preliminary predictions for diffractive Higgs production at the Tevatron and LHC are introduced. It is hinted that the cross sections for diffractive Higgs at the Tevatron are uninterestingly small, but become significant at the higher energies of LHC.

The special events with rapidity gaps between jets are shortly discussed. Due to the large momentum transfer across the rapidity gap, the soft colour models cannot give a satisfactory explanation. Good agreement with data is obtain if one considers a colour singlet exchange, based on a complete solution to the BFKL equation, including non-leading corrections. The soft colour effects are used to provide a dynamical gap survival probability, which varies from event to event.

Paper IV

In this Letter we report on the possibilities of observing the Higgs boson in diffractive events. It has been argued in the literature that the Higgs can be more easily reconstructed from its decay products in diffractive events at high energy colliders, based on the lower hadronic activity in the events with rapidity gaps.

Based on the success of the soft colour interaction models in describing all hard diffractive data from HERA and the Tevatron, our models can provide reliable predictions for diffractive Higgs production.

The rate of diffractive Higgs events with one or two leading particles (or corresponding gaps) is too low at the Tevatron to be useful, for a Higgs with a mass $115 < m_H < 200$ GeV. In contrast, the high energy and luminosity of the LHC will facilitate the study of diffractive Higgs production, and events with two leading protons can be observed.

We also find that diffractive events at LHC are not as clean as expected, since the large available energy is enough to produce a hard system containing the Higgs, one or two leading protons, and still populate the forward detector rapidity region with particles.

Paper V

This paper gives a summary of the predictions for different diffractive processes, made using the soft colour interaction models. The predicted ratios for diffractive Z production are in good agreement with those recently found at the Tevatron (see Table 5.1).

The predictions for diffractive Higgs at the Tevatron are discussed, with emphasis on production of a central system in rapidity containing the Higgs boson,

accompanied by two leading particles or rapidity gaps.

A process with similar dynamics has already been observed in $p\bar{p}$ collisions [67], events having a hard ($p_\perp > 7$ GeV) dijet system located central in rapidity, with a leading antiproton and a gap on the proton side.

The soft colour interaction models describe well the cross sections of the latter process at the Tevatron (Paper II), as well as more exclusive quantities such as distributions in transverse energy and rapidity of the jets. In this paper, another measurement is well described by the SCI model, the distribution in the dijet mass fraction (fraction of the available energy in the central system of DPE events, that goes into the production of the two jets). This success gives confidence in the prediction for diffractive Higgs with two leading protons, with too low cross section at the Tevatron, but a visible one at the LHC.

Paper VI

This paper deepens the study of diffractive Higgs production at hadrons colliders and it introduces predictions for diffractive production of prompt photon pairs.

One crucial issue is whether the cross section for diffractive Higgs production is large enough. Another issue is which decay mode for Higgs is considered. Although $H \to \gamma\gamma$ has a small branching ratio, it gives a very clear experimental signature and is often considered for a Higgs of intermediate mass ($115 < m_H < 160$ GeV).

The study of diffractive prompt photons is interesting because the production process $gg \to \gamma\gamma$ is similar to the dominating Higgs production process $gg \to H$, involving a quark loop. Thus, the experimental observation of prompt photon pairs in rapidity gap events can be used to test the models for diffractive Higgs production, and in this paper predictions are given for single diffractive and DPE events at both the Tevatron and LHC.

Furthermore, we find that photon pair production provides a dominating irreducible background for $H \to \gamma\gamma$, implying that other decay modes of the Higgs have to be used in order to study single diffractive and DPE Higgs at hadron colliders.

5.2 Photon structure and $\gamma\gamma$ interactions

The photon is one of the basic elementary particles with properties that follow from the Standard Model. It is a massless, chargeless object with a point-like coupling to the charged fundamental particles. As such, it provides an ideal tool for probing the structure of more complicated objects, like hadrons.

The concept of the structure of the photon is very natural in quantum field theory, since the photon can fluctuate into various states with the same quantum numbers. These virtual states may consist of mesons, lepton-antilepton pairs, quark-antiquark pairs, etc., which can be realised due to an interaction providing the necessary energy-momentum to make the state become real.

In soft photon-hadron interactions, similarities between the interactions of a photon and those of the vector mesons ρ, ω, ϕ have been observed, making the hadronic properties of the photon more apparent.

In perturbative QCD, the fluctuation $\gamma \to q\bar{q}$ leads to the partonic structure of the photon. This can be probed in an analogous way as testing the structure of hadronic objects – using a hard probe, often provided by another photon.

Since in the present experiments there are no beams of high-energy real photons, testing the structure of the photon is performed at the e^+e^- colliders or $e^{\pm}p$ colliders. In both cases, the flux of initial photons arises from the electron or positron beams through bremsstrahlung, and can be calculated using the Weizsäcker-Williams approximation. Thus, one can study the properties of the photon in $e\gamma$ deep inelastic scattering and $\gamma\gamma$ collisions, or in γp collisions (called photoproduction).

In the past two decades, a wide range of experimental measurements have been performed on photon-photon interactions and photon structure. The cross sections for collisions of $\gamma\gamma$ [68] and $\gamma^*\gamma^*$ [69] of different virtualities are known for high energies (~ 200 GeV), as well as the photon structure functions [70] for a wide range of Q^2 and x.

The photon structure provides one of the basic tests of QCD, since QCD can give definite predictions for the structure function of the photon and its logarithmic rise with Q^2, or the large quark densities in the photon for large values of x. The direct coupling of the photon to the quarks makes the process fully calculable in QCD, providing an advantage over the case of proton structure.

The photon interactions, and in particular $\gamma^*\gamma^*$ interactions, also offer a good testing ground for QCD resummation techniques at high energies. The concept of parton density saturation is a recent development of QCD theory and phenomenology, and it can also be tested in photon interactions (Papers VII and VIII).

Additional information on the structure of the photon is coming from the production of heavy quarks in photon-induced processes [71, 72]. In such processes, the heavy quark mass provides in a natural way the hard scale allowing the application of perturbative QCD. A large discrepancy was found for bottom production in $\gamma\gamma$ collisions [72], between the measured cross section and the QCD predictions. Similar enhancements of bottom production have been reported in γp and $p\bar{p}$ collisions, suggesting the presence of an important systematic effect omitted in the QCD analysis. Taking into account gluon transverse momenta in the framework of k_t factorization could provide an answer (Paper IX).

Paper VII

This paper extends the basic principles of the GBW saturation model to describe $\gamma^*\gamma^*$ scattering cross section, providing a test of the saturation model in a new environment and confirming the universality of the model.

The $\gamma^*\gamma^*$ scattering is described within the formalism of two interacting colour

dipoles into which the virtual photons fluctuate (Fig. 5.1). The interaction between the two dipoles is modelled to incorporate the saturation property, with the saturation radius $R_0(x)$ taken from the GBW analysis of the $\gamma^* p$ interactions at HERA.

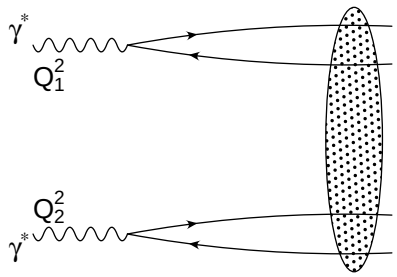

Figure 5.1: Diagram illustrating $\gamma^*\gamma^*$ interactions in the dipole representation.

This approach makes it possible to describe in a unified way the variations of the energy dependence of the cross section with the change of the virtualities of the photons (Q_1^2 and Q_2^2).

With a suitable choice of quark masses, the model gives a very good description of the observed $\gamma\gamma$ total cross section (both photons are real), the $\gamma^*\gamma^*$ total cross section for two virtual photons and the photon structure function $F_2^\gamma(x, Q^2)$ of a real photon, for low values of x (measured in $\gamma^*\gamma$ interactions).

In the region where the saturation effects become important, the model gives a steeper dependence of the cross section on the collision energy than that obtained in the case of $\gamma^* p$ scattering, as confirmed by the experimental observations.

The production of heavy quarks in $\gamma\gamma$ interactions is also studied, with a reasonable description of observed production of charm quarks, but insufficient for bottom production. We also present predictions of the model for the very high energy range which will be investigated at future linear colliders.

Paper VIII

This paper briefly presents the saturation model for photon-photon interactions, based on a QCD dipole picture of high energy interactions, where the two-dipole cross section is assumed to satisfy the saturation property.

The saturation model accounts for an exchange of gluonic degrees of freedom, which dominate at high energies. In order to get a complete description of the photon-photon interactions, the terms important at low energy are added, *i.e.* the so called quark-box contribution when both photons couple to a quark loop (similar to Fig. 5.2a), and non-perturbative contributions related to Regge trajectories of light mesons.

In this paper, the main results of the model are summarised. The model gives a very good description of the experimental data on $\gamma\gamma$, $\gamma^*\gamma^*$ and $\gamma^*\gamma$ interactions.

Paper IX

This paper approaches the production of heavy quarks in photon-photon interactions through the k_t factorization formalism. This approach is motivated by the observed enhancement in the calculations of the cross section for bottom production in $p\bar{p}$ collisions due to the inclusion of non-zero transverse momenta of the gluons, as compared to the collinear formalism.

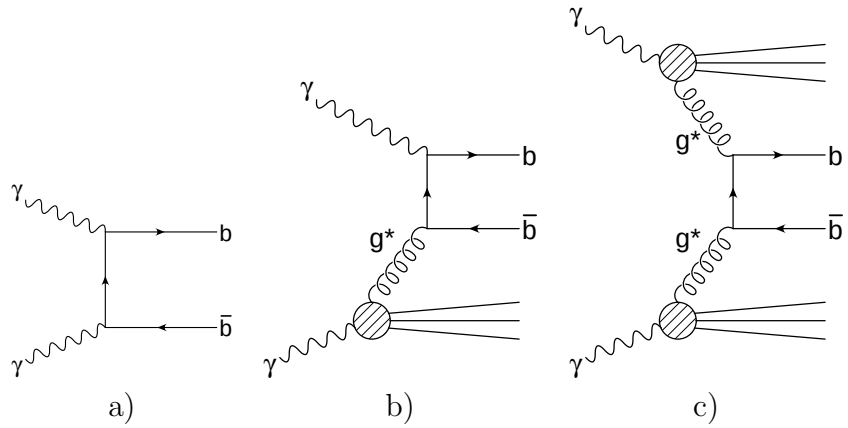

Figure 5.2: Bottom production in $\gamma\gamma$ collisions through different mechanisms: a) direct production, b) one photon is resolved and c) both photons are resolved.

The unintegrated gluon distribution $\mathcal{F}_g(x, k_t^2, \mu^2)$ in the photon is determined using the Kimber-Martin-Ryskin (KMR) [73] prescription, which gives $\mathcal{F}_g(x, k_t^2, \mu^2)$ as an approximate solution to the CCFM equation. In addition, a model of the unintegrated gluon density is proposed based on the saturation model extended to the region of large x values.

Using the k_t factorization approach, the above gluon densities are applied to obtain the cross sections for charm and bottom production in γp, and for the first time in $\gamma\gamma$ collisions. We investigate both direct and resolved photon contributions (see Fig. 5.2) and make a comparison with the results obtained in the collinear approach and the experimental data.

While the charm production cross section is found to be consistent with the experimental data for both $\gamma^* p$ and $\gamma\gamma$ collisions, the estimates obtained for bottom are below the observed cross sections. Due to theoretical and experimental uncertainties, one cannot claim a significant disagreement for bottom production in γp collisions, but a substantial discrepancy of bottom production in photon-photon collisions still remains.

5.3 BRST quantization of reducible theories

The BRST formalism provides a very powerful method of quantization for gauge theories. The advantage of this formalism over other quantization methods (for

example Faddeev-Popov approach) is that it can be applied to irreducible as well as reducible gauge theories.

Irreducible theories are the simplest gauge theories for which all gauge transformations are independent. An example of an irreducible theory is Yang-Mills theory, and one can see in Eq. (4.2) that the generators of the gauge transformations are all independent. This theory can be quantized using Faddeev-Popov approach, or the antifield BRST formalism, and the result will be the appearance of ghost fields, corresponding to the gauge transformations.

In reducible theories, the gauge generators are not independent. These theories involve a redundant set of gauge invariances, so there are relations among the gauge generators. These relations can be thought of as 'gauge invariance' for gauge invariance. Furthermore, these new relations might not be independent as well, leading to a complex structure of the gauge theory (for example the open bosonic string field theory).

Modifications of the Faddeev-Popov procedure have been developed by introducing the so called ghosts of ghosts, which will correspond to the new gauge invariances. Such modifications do not work, however, for general reducible theories, and the BRST formalism is the only one which can systematically quantize these theories.

A reducible theory is called first-stage reducible if the relations between the gauge generators are independent. Examples of such theories are the spin-5/2 gauge theory (Paper X) and the topological Yang-Mills theory (Paper XI). If there are several stages of reducibility, where every obtained relation for the 'gauge invariances' can be further reduced, one talks about L-stage reducible theories. The open bosonic string is an infinite-stage reducible system.

The first-stage reducible theories can be quantized in the BRST formalism, following a simple idea of transforming the reducible system into an irreducible one [58]. This system can then be quantized using the irreducible BRST approach, as presented in Chapter 4.

Paper X

This paper presents the quantization of massless spin-5/2 gauge theory in an irreducible manner using the BRST formalism. This theory has a remarkable gauge symmetry and, through its connection to string theory, provides a promising candidate for building a unified physical theory.

Although this theory is first-stage reducible, it can be quantized using the BRST approach without introducing ghosts of ghosts. This is achieved by introducing some fields with the help of which the reducible gauge generators will be replaced with irreducible ones.

These fields have trivial field equations, carry spin 1/2 and are associated with the relations between the gauge generators. The action containing these fields is invariant under the gauge transformations of the spin-5/2 fields and the spin-1/2 fields, and these gauge transformations are independent. Thus, an irreducible

system has been constructed. The physical observables of the original reducible theory and the new irreducible theory coincide.

The irreducible theory is quantized using the antifield BRST formalism and different gauge fixing procedures are discussed. Also the BRST-anti-BRST [74] procedure is used to quantize this theory and a consistent result is found.

Paper XI

The quantization of the topological Yang-Mills theory is presented using the irreducible BRST approach. The topological Yang-Mills is a first-stage reducible theory and it provides an interesting test of the BRST machinery, since both the gauge generators and the reducibility functions depend on the gauge fields.

Furthermore, it is believed that topologically non-trivial configurations play a dominant role in phenomena like the quark confinement in QCD. In particular, the topological Yang-Mills theories could be embedded in the ordinary Yang-Mills theories to account for the non-perturbative sectors of the theory.

The idea behind the quantization of topological Yang-Mills theory is to transform the reducible gauge transformations into some irreducible ones by means of enlarging the original field spectrum with scalar fields. For every reducibility relation a new field with a gauge transformation is added. The fields are introduced such that the physical content of the system remains unaltered.

The obtained irreducible theory is quantized using two approaches, the antifield BRST method and the Hamiltonian BRST approach [58]. The two approaches are shown to lead to the same path integral, thus verifying their equivalence.

Publications not included in the thesis:

XII G. Ingelman, A. Edin, R. Enberg, J. Rathsman and N. Tîmneanu,
Rapidity gaps from colour string topologies,
Nuclear Physics Proceedings Supplement B **79** (1999) 386,
hep-ph/9912535.

XIII G. Ingelman, A. Edin, R. Enberg, J. Rathsman and N. Tîmneanu,
Soft colour interactions in non-perturbative QCD,
Nuclear Physics A **663** (2000) 1007, hep-ph/9912537.

XIV R. Enberg, G. Ingelman and N. Tîmneanu,
Rapidity gaps at HERA and the Tevatron from soft colour exchanges,
Journal of Physics G **26** (2000) 712, hep-ph/0001016.

XV J. Kwieciński, L. Motyka and N. Tîmneanu,
Two-photon cross-sections from the saturation model,
Acta Physica Polonica B **33** (2002) 1559, hep-ph/0206129.

Chapter 6

Conclusions and outlook

The experimental success and consistent theoretical construction of the Standard Model has established it as the "Standard Theory" of particle physics. It describes the fundamental constituents of matter, quarks and leptons, and the interactions among these, describing in a common framework the electromagnetic, weak and strong interactions. The Higgs boson, yet undiscovered, is the missing link which keeps the Standard Model from being complete.

An important sector of the Standard Model, consisting of quarks and gluons, is described by Quantum Chromodynamics, which is now established as the theory of strong interactions. After its great success in describing a wealth of experimental data at high energies, QCD is no longer under scrutiny for testing it as the relevant theory, but for testing our understanding of it. There is still one major missing piece in our understanding of QCD – confinement. Why cannot quarks and gluons exist as isolated particles in nature, but are instead confined in hadrons?

Understanding confinement is a "million dollar" question, an open problem at the beginning of the century. While the discovery of the Higgs boson is an experimental challenge, which is undertaken at the present and future particle accelerators, the understanding of confinement is a theoretical challenge.

Confinement is related to the long distance part of strong interactions, *i.e.* QCD in soft interactions. The interplay between soft and hard physics offers a way to investigate such soft dynamics, using well known perturbative QCD as a basis. This thesis is exploring the hard-soft interplay in QCD with the goal of extending our understanding of the strong interactions. Different aspects of these interactions mediated by gluons emerge from the various approaches used in this thesis.

The soft colour interaction models deepen our understanding and description of hadronization. In hard interactions, *soft gluon exchanges* can rearrange the colour structure of the final state, leading to a different observable final state. This thesis shows how the soft colour interaction models successfully describe all observations on diffractive hard processes in deep inelastic scattering and hadron-hadron collisions. The models have predictive power, and the thesis also presents the prospects of observing Higgs bosons or prompt photons in this type of events.

Insight into the photon structure and photon interactions at high energies can be obtained based on new ideas about gluon interactions. *Multiple gluon exchanges* in photon-proton collisions at high energies have been associated with saturation. This idea has been extended in this thesis to photon-photon collisions, and good agreement with experimental data has been obtained. Another new idea concerning the distributions of virtual gluons inside a hadron has in this thesis been considered for the photon, resulting in the first parameterizations for *off-shell gluon distributions*. These distributions can be used for calculations of different processes involving incoming photons, where the effects of gluon transverse momenta are important, for example production of heavy quarks.

The BRST method of quantization has proven to be a very powerful method of quantizing gauge theories. This thesis explores the benefits of this method on different gauge theories with a more complex gauge structure than QCD. Such theories could provide promising candidates for unified physical theories (spin-5/2 theories), or shed light on the non-perturbative sector of QCD (topological Yang-Mills theories).

Although the Standard Model is very successful, there are still some fundamental questions without an answer. Why are there three generations of fundamental particles? If the Higgs particle is not found, what is the mechanism for mass generation? How can gravity be unified with the other fundamental forces? There are reasons to believe that the Standard Model will be insufficient at higher energies than those available today and that future colliders might discover new physics. The new physics could hold the answer to these questions, in terms of supersymmetry, extra spatial dimensions or string theory.

As for the longstanding fundamental problem of QCD – confinement – a solution might emerge in the future from several approaches based on first principles. One of them is the translation of QCD to a discretized euclidian version of the theory with the aim of performing lattice calculations [75]. The understanding of non-perturbative non-abelian gauge theories might be obtained in the framework of AdS/CFT correspondence (Anti de Sitter/Conformal Field Theory) [76, 77] between the string theory and Yang-Mills theory.

The studies of gluon dynamics presented in this thesis have increased our knowledge of strong interactions, and will contribute to a future understanding of all aspects of QCD.

Acknowledgements

I would like to express my sincere gratitude to my supervisor Gunnar Ingelman for his continuous guidance, support and encouragement. My warmest thanks for introducing me to the fascinating world of particle physics and for offering me the opportunity to become part of it. Many thanks also for all that you taught me and for the possibilities to actively participate in the academic and international particle physics community, at summer schools and conferences.

I wish to give zillions of thanks to my close colleague and friend Rikard Enberg for endless and sometimes speculative, yet useful discussions, for a fruitful collaboration and a great time. I learned very much from Leszek Motyka, whom I wish to send my heartfelt thanks for his continuous encouragement, and for enlightening and productive discussions.

My sincere thanks to Johan Rathsman for all scientific discussions about Monte Carlo generators, soft interactions and more, and I thank both him and Anders Edin for their valuable help at the beginning of my studies. I would also like to thank Jan Kwieciński for his guidance on different theoretical aspects of photon physics. I am indebted to Constantin Bizdadea and Odile Saliu at the University of Craiova, Romania, for initiating me in research in theoretical physics.

My thanks go to all at the department for the nice working atmosphere. My special thanks to Inger Ericson and Ib Koersner for their help and for rescuing me from under the pile of official papers or computer files and cables.

Many thanks to the present and former students in the theory group and the High Energy Physics division – we learned a lot from each other and had many memorable moments. Dear Kristel, Rikard, Mattias and Marek, I greatly appreciate our friendship.

Closer to the heart are my parents and I thank them for always believing in me. It gives me great pleasure to thank Gunnar and Birgitta Tibell, whose hearts and door are always open.

Last, but certainly not least, my soulmate and beloved wife Anca receives my pure thoughts and thanks: “ce bine ca esti, ce mirare ca sunt!”.

List of acronyms and abbreviations

BFKL	Balitsky-Fadin-Kuraev-Lipatov
BRST	Becchi-Rouet-Stora-Tyutin
CCFM	Ciafaloni-Catani-Fiorani-Marchesini
CERN	Conseil Européen pour la Recherche Nucléaire
CTEQ	Coordinated Theoretical-Experimental project on QCD
DESY	Deutsches Elektronen-Synchrotron
DGLAP	Dokshitzer-Gribov-Lipatov-Altarelli-Parisi
DIS	Deep Inelastic Scattering
DPE	Double Pomeron Exchange / Double leading Proton Event
EW	Electro-Weak
GAL	Generalized Area Law
GBW	Golec-Biernat and Wüsthoff
HERA	Hadron Elektron Ringanlage
KMR	Kimber-Martin-Ryskin
LEP	Large Electron-Positron collider
LHC	Large Hadron Collider
LO	Leading Order
ME	Matrix Elemets
MI	Multiple Interactions
NLO	Next-to-Leading Order
OPE	Operator Product Expansion
PDF	Parton Distribution Function
PDG	Particle Data Group
pQCD	perturbative Quantum Chromodynamics
QCD	Quantum Chromodynamics
QED	Quantum Electrodynamics
RGE	Renormalization Group Equations
SCI	Soft Colour Interaction
SD	Single Diffraction
SLAC	Stanford Linear Accelerator Center
SM	Standard Model

Bibliography

[1] K. Hagiwara *et al.* [Particle Data Group Collaboration], Phys. Rev. D **66** (2002) 010001.

[2] P. W. Higgs, Phys. Lett. **12** (1964) 132;
P. W. Higgs, Phys. Rev. Lett. **13** (1964) 508;
P. W. Higgs, Phys. Rev. **145** (1966) 1156;
F. Englert and R. Brout, Phys. Rev. Lett. **13** (1964) 321.

[3] [LEP Higgs Working Group for Higgs boson searches Collaboration], hep-ex/0107029.

[4] T. Regge, Nuovo Cim. **14** (1959) 951.

[5] M. Gell-Mann, Phys. Lett. **8** (1964) 214.

[6] G. Zweig, CERN-TH-401 and CERN-TH-412.

[7] O. W. Greenberg, Phys. Rev. Lett. **13** (1964) 598.

[8] M. Y. Han and Y. Nambu, Phys. Rev. **139** (1965) B1006.

[9] E. D. Bloom *et al.*, Phys. Rev. Lett. **23** (1969) 930;
M. Breidenbach *et al.*, Phys. Rev. Lett. **23** (1969) 935.

[10] R. P. Feynman, Phys. Rev. Lett. **23** (1969) 1415.

[11] J. D. Bjorken and E. A. Paschos, Phys. Rev. **185** (1969) 1975.

[12] C. N. Yang and R. L. Mills, Phys. Rev. **96** (1954) 191.

[13] L. D. Faddeev and V. N. Popov, Phys. Lett. B **25** (1967) 29.

[14] G. 't Hooft, Nucl. Phys. B **33** (1971) 173;
G. 't Hooft, Nucl. Phys. B **35** (1971) 167;
G. 't Hooft and M. J. Veltman, Nucl. Phys. B **44** (1972) 189;
G. 't Hooft and M. J. Veltman, Nucl. Phys. B **50** (1972) 318.

[15] D. J. Gross and F. Wilczek, Phys. Rev. Lett. **30** (1973) 1343.

[16] H. D. Politzer, Phys. Rev. Lett. **30** (1973) 1346.

[17] H. Fritzsch, M. Gell-Mann and H. Leutwyler, Phys. Lett. B **47** (1973) 365.

[18] M. Gell-Mann, Phys. Rev. **125** (1962) 1067.

[19] S. Weinberg, Phys. Rev. Lett. **31** (1973) 494.

[20] D. J. Gross and F. Wilczek, Phys. Rev. D **8** (1973) 3633.

[21] D. J. Gross and F. Wilczek, Phys. Rev. D **9** (1974) 980.

[22] H. Georgi and H. D. Politzer, Phys. Rev. D **9** (1974) 416.

[23] Y. Watanabe *et al.*, Phys. Rev. Lett. **35** (1975) 898;
C. Chang *et al.*, Phys. Rev. Lett. **35** (1975) 901.

[24] K. G. Wilson, Phys. Rev. **179** (1969) 1499.

[25] J. J. Aubert *et al.*, Phys. Rev. Lett. **33** (1974) 1404;
J. E. Augustin *et al.*, Phys. Rev. Lett. **33** (1974) 1406.

[26] S. W. Herb *et al.*, Phys. Rev. Lett. **39** (1977) 252.

[27] T. Appelquist and H. D. Politzer, Phys. Rev. Lett. **34** (1975) 43.

[28] G. Sterman and S. Weinberg, Phys. Rev. Lett. **39** (1977) 1436.

[29] C. Berger *et al.* [PLUTO Collaboration], Phys. Lett. B **86** (1979) 418;
W. Bartel *et al.* [JADE Collaboration], Phys. Lett. B **91** (1980) 142;
W. Braunschweig *et al.* [TASSO Collaboration], Z. Phys. C **47** (1990) 187.

[30] K. G. Wilson, Phys. Rev. D **10** (1974) 2445.

[31] J. B. Kogut and L. Susskind, Phys. Rev. D **11** (1975) 395.

[32] M. Creutz, "Quarks, Gluons and Lattices," Cambridge University Press (1983).

[33] R. Brock *et al.* [CTEQ Collaboration], Rev. Mod. Phys. **67** (1995) 157.

[34] T. Muta, "Foundations of Quantum Chromodynamics," World Scientific (1998).

[35] R. K. Ellis, W. J. Stirling, B. R. Webber, "QCD and Collider Physics," Cambridge University Press (1996).

[36] Yu. L. Dokshitzer, V. A. Khoze, A. H. Mueller, S. I. Troyan, "Basics of Perturbative QCD," Edition Frontiers (1991).

[37] W. Heisenberg and W. Pauli, Z. Phys. **56** (1929) 1;
W. Heisenberg and W. Pauli, Z. Phys. **59** (1930) 168.

[38] R. P. Feynman, Rev. Mod. Phys. **20** (1948) 367.

[39] H. Lehmann, K. Symanzik and W. Zimmermann, Nuovo Cim. **1** (1955) 205.

[40] E. C. Stueckelberg and A. Petermann, Helv. Phys. Acta **26** (1953) 499.

[41] M. Gell-Mann and F. E. Low, Phys. Rev. **95** (1954) 1300.

[42] A. Edin and G. Ingelman, Phys. Lett. B **432** (1998) 402.

[43] V. N. Gribov and L. N. Lipatov, Sov. J. Nucl. Phys. **15** (1972) 438;
V. N. Gribov and L. N. Lipatov, Sov. J. Nucl. Phys. **15** (1972) 675;
L. N. Lipatov, Sov. J. Nucl. Phys. **20** (1975) 94;
G. Altarelli and G. Parisi, Nucl. Phys. B **126** (1977) 298;
Y. L. Dokshitzer, Sov. Phys. JETP **46** (1977) 641.

[44] L. N. Lipatov, Sov. J. Nucl. Phys. **23** (1976) 338;
E. A. Kuraev, L. N. Lipatov, V. S. Fadin, Sov. Phys. JETP **44** (1976) 443;
E. A. Kuraev, L. N. Lipatov, V. S. Fadin, Sov. Phys. JETP **45** (1977) 199;
I. I. Balitsky and L. N. Lipatov, Sov. J. Nucl. Phys. **28** (1978) 822.

[45] B. Andersson, G. Gustafson, G. Ingelman and T. Sjöstrand, Phys. Rept. **97** (1983) 31.

[46] J. C. Collins, D. E. Soper, and G. Sterman, in "Perturbative Quantum Chromodynamics", ed. A. H. Mueller, World Scientific (1989), 1.

[47] G. Ingelman, A. Edin and J. Rathsman, Comput. Phys. Commun. **101** (1997) 108.

[48] T. Sjöstrand, P. Edén, C. Friberg, L. Lönnblad, G. Miu, S. Mrenna and E. Norrbin, Comput. Phys. Commun. **135** (2001) 238.

[49] A. Edin, G. Ingelman and J. Rathsman, Phys. Lett. B **366** (1996) 371;
A. Edin, G. Ingelman and J. Rathsman, Z. Phys. C **75** (1997) 57.

[50] J. Rathsman, Phys. Lett. B **452** (1999) 364.

[51] K. Golec-Biernat and M. Wüsthoff, Phys. Rev. D **59** (1999) 014017;
K. Golec-Biernat and M. Wüsthoff, Phys. Rev. D **60** (1999) 114023.

[52] M. Ciafaloni, Nucl. Phys. B **296** (1988) 49;
S. Catani, F. Fiorani and G. Marchesini, Phys. Lett. B **234** (1990) 339;
S. Catani, F. Fiorani and G. Marchesini, Nucl. Phys. B **336** (1990) 18;
G. Marchesini, Nucl. Phys. B **445** (1995) 49.

[53] S. Catani, M. Ciafaloni and F. Hautmann, Nucl. Phys. B **366** (1991) 135;
J. C. Collins and R. K. Ellis, Nucl. Phys. B **360** (1991) 3.

[54] L. V. Gribov, E. M. Levin and M. G. Ryskin, Phys. Rept. **100** (1983) 1;
E. M. Levin, M. G. Ryskin, Y. M. Shabelski and A. G. Shuvaev, Sov. J. Nucl. Phys. **53** (1991) 657.

[55] C. Becchi, A. Rouet and R. Stora, Phys. Lett. B **52** (1974) 344;
C. Becchi, A. Rouet and R. Stora, Commun. Math. Phys. **42** (1975) 127;
C. Becchi, A. Rouet and R. Stora, Annals Phys. **98** (1976) 287;
I. V. Tyutin, Lebedev preprint LEBEDEV-75-39 (1975), unpublished.

[56] I. A. Batalin and G. A. Vilkovisky, Phys. Lett. B **69** (1977) 309;
I. A. Batalin and G. A. Vilkovisky, Phys. Lett. B **102** (1981) 27;
I. A. Batalin and G. A. Vilkovisky, Phys. Lett. B **120** (1983) 166;
I. A. Batalin and G. A. Vilkovisky, Phys. Rev. D **28** (1983) 2567 [Erratum-ibid. D **30** (1984) 508];
I. A. Batalin and G. A. Vilkovisky, Nucl. Phys. B **234** (1984) 106;
I. A. Batalin and G. A. Vilkovisky, J. Math. Phys. **26** (1985) 172.

[57] M. Henneaux, Phys. Lett. B **313** (1993) 35 [Err.-ibid. B **316** (1993) 633].

[58] M. Henneaux and C. Teitelboim, "Quantisation of Gauge Systems", Princeton University Press, Princeton (1992).

[59] J. Gomis, J. Paris and S. Samuel, Phys. Rept. **259** (1995) 1.

[60] G. Ingelman and P. E. Schlein, Phys. Lett. B **152** (1985) 256.

[61] R. Bonino *et al.* [UA8 Collaboration], Phys. Lett. B **211** (1988) 239.

[62] M. Derrick *et al.* [ZEUS Collaboration], Phys. Lett. B **315** (1993) 481;
M. Derrick *et al.* [ZEUS Collaboration], Z. Phys. C **68** (1995) 569;
T. Ahmed *et al.* [H1 Collaboration], Nucl. Phys. B **429** (1994) 477;
T. Ahmed *et al.* [H1 Collaboration], Phys. Lett. B **348** (1995) 681.

[63] A. Edin, G. Ingelman and J. Rathsman, Phys. Rev. D **56** (1997) 7317.

[64] F. Abe *et al.* [CDF Collaboration], Phys. Rev. Lett. **74** (1995) 855;
F. Abe *et al.* [CDF Collaboration], Phys. Rev. Lett. **80** (1998) 1156;
F. Abe *et al.* [CDF Collaboration], Phys. Rev. Lett. **81** (1998) 5278;
B. Abbott *et al.* [D0 Collaboration], Phys. Lett. B **440** (1998) 189.

[65] R. Enberg, G. Ingelman and L. Motyka, Phys. Lett. B **524** (2002) 273.

[66] T. Affolder *et al.* [CDF Collaboration], Phys. Rev. Lett. **84** (2000) 5043.

[67] T. Affolder *et al.* [CDF Collaboration], Phys. Rev. Lett. **85** (2000) 4215.

[68] G. Abbiendi *et al.* [OPAL Collaboration], Eur. Phys. J. **C14** (2000) 199;
M. Acciarri *et al.* [L3 Collaboration], Phys. Lett. **B519** (2001) 33.

[69] M. Acciarri *et al.* [L3 Collaboration], Phys. Lett. **B453** (1999) 333;
G. Abbiendi *et al.* [OPAL Collaboration], hep-ex/0110006.

[70] M. Acciarri *et al.* [L3 Collaboration], Phys. Lett. **B436** (1998) 403;
M. Acciarri *et al.* [L3 Collaboration], Phys. Lett. **B447** (1999) 147;
G. Abbiendi *et al.* [OPAL Collaboration], Eur. Phys. J. **C18** (2000) 15;
R. Barate *et al.* [ALEPH Collaboration], Phys. Lett. **B458** (1999) 152;
P. Abreu *et al.* [DELPHI Collaboration], Z. Phys. **C69** (1996) 223.

[71] M. Acciarri *et al.* [L3 Collaboration], Phys. Lett. **B514** (2001) 19.

[72] M. Acciarri *et al.* [L3 Collaboration], Phys. Lett. B **503** (2001) 10;
The OPAL Collaboration, OPAL Physics Note PN455.

[73] M. A. Kimber, A. D. Martin and M. G. Ryskin, Phys. Rev. D **63** (2001) 114027.

[74] I. A. Batalin, P. M. Lavrov and I. V. Tyutin, J. Math. Phys. **31** (1990) 1487;
P. Gregoire and M. Henneaux, J. Phys. A **26** (1993) 6073.

[75] H. Wittig, arXiv:hep-ph/9911400.

[76] J. M. Maldacena, Adv. Theor. Math. Phys. **2** (1998) 231 [Int. J. Theor. Phys. **38** (1999) 1113].

[77] R. A. Janik and R. Peschanski, Nucl. Phys. B **549** (1999) 280;
R. A. Janik and R. Peschanski, Nucl. Phys. B **565** (2000) 193;
R. A. Janik and R. Peschanski, Nucl. Phys. B **586** (2000) 163;
R. A. Janik, Phys. Lett. B **500** (2001) 118.